Understanding the transmission pathways of Lassa fever: A mathematical modeling approach

Praise-God Uchechukwu Madueme, Faraimunashe Chirove[*]

Department of Mathematics and Applied Mathematics, University of Johannesburg, Cnr Kingsway and University Road, Auckland Park, 2092, Johannesburg, South Africa

ARTICLE INFO

ABSTRACT

The spread of Lassa fever infection is increasing in West Africa over the last decade. The impact of this can better be understood when considering the various possible transmission routes. We designed a mathematical model for the epidemiology of Lassa Fever using a system of nonlinear ordinary differential equations to determine the effect of transmission pathways toward the infection progression in humans and rodents including those usually neglected such as the environmental surface and aerosol routes. We analyzed the model and carried out numerical simulations to determine the impact of each transmission routes. Our results showed that the burden of Lassa fever infection is increased when all the transmission routes are incorporated and most single transmission routes are less harmful, but when in combination with other transmission routes, they increase the Lassa fever burden. It is therefore important to consider multiple transmission routes to better estimate the Lassa fever burden optimally and in turn determine control strategies targeted at the transmission pathways.

1. Introduction

Lassa fever (LF) is an acute viral zoonotic illness responsible for a severe hemorrhagic fever. It is an illness caused by Lassa virus which is a single-stranded RNA virus from the arenavirus family. It was first discovered in 1969 in a Nigerian town called Lassa in Borno State when two missionary nurses died from the illness (Richmond & Baglole, 2003). The animal vector of this virus is the multimammate rat (*Mastomys natalensis*) which is one of the most common rodents in West Africa (CDC, 2014; Gonzalez, 2020; NICD, 2020). The *Mastomys* rodents reproduce often and excrete the virus in urine for a very long period of time, and because they occupy human homes, especially where food is stored, they help spread the virus to humans. The transmission of this virus to humans can be through direct or indirect contact. Direct transmissions result from contact between humans and humans, rodents and humans, and rodents and rodents. The evidence available shows that human to human transmission occurs through contact with the body fluids, secretions, excretions, blood of the infectious individual, and sexual transmission (Newman, 2018; NICD, 2020). The infected *Mastomys* rodents are caught (as bush meat) and eaten as food in certain places which directly infects the individuals with the virus. Reports have also shown that there is both

---

horizontal and vertical transmission in multimammate rats especially in seasons when these rodents are actively breeding (Fichet-Calvet et al., 2014; Tewogbola & Aung, ; Gibb et al., 2017). In this paper, however, vertical transmission from rodent to rodent is not covered. Rodents can deposit the virus through their urine and faeces on surfaces in the households such as walls and places where food is stored or even on surfaces where medical equipment is kept. Humans can indirectly acquire the virus when they come in contact with the virus on these contaminated surfaces. Rodents can also become infected because rats share garbage, food on surfaces contaminated with the excretions of infectious rodents yet do not die due to disease but carry the infection and continue to shed it throughout their lifetime (NICD, 2020; Obabiyi & Onifade, 2017). Another form of indirect transmission is through airborne (aerosol) transmission which occurs especially in health centres when people inhale air particles contaminated with the droppings of infected rodents especially during activities like sweeping and other wind activities (CDC, 2014; Gonzalez, 2020; NICD, 2020). The natural history of Lassa fever reveals that its transmission pattern is driven by the frequency of exposure to infected individuals or through contact with infected rodents and contaminated environments (Akhmetzhanov et al., 2019; Sabeti, 2015). It has been shown that Lassa virus is stable as an aerosol, particularly at low relative humidity (30% RH) and the biological half-life at both 24 °C and 32 °C ranges from 10.1 to 54.6 min (CDC, 2014; Stephenson et al., 1984).

Frequent cases of Lassa virus infection have been seen in endemic regions such as Nigeria, Benin, Ghana, Guinea, Liberia, Mali, Sierra Leone and Togo. Surrounding regions like Central African Republic, Burkina Faso, Côte d'Ivoire, Mali, Senegal, Ghana among others are also at risk, because the rodents that transmit the virus are very common throughout West and East Africa. Hospital staff are also at risk for infection especially in areas with inadequate protective measures and improper sterilization methods (Gibb et al., 2017; NICD, 2020; WHO, 2017). After contracting the virus, humans show symptoms between 1 and 3 weeks. The presence of virus in the blood is known to peak four to nine days after the onset of symptoms. In most cases, 80% of people infected show no observable or mild symptoms. For these individuals, they show mild signs like slight fever, general malaise and weakness, and headache but do not die due to the infection. Recovery can take place eight to ten days after inception. The remaining 20% of infected individuals can show more severe symptoms like bleeding in the gums, eyes, or nose, respiratory distress, repeated vomiting, facial swelling, pain in the chest, back, and abdomen, shock, and failure in body organs such as liver, spleen and kidneys. The virus in this group of people may also lead to complications such as hearing loss, tremors, encephalitis or even death within 2 weeks after the onset of symptoms due to multiple organ failure (CDC, 2014; WHO, 2017; Yun & Walker, 2012). The number of Lassa virus infections per year in West Africa is estimated at 100,000 to 300,000, with approximately 5000 deaths. In some places in Liberia and Sierra Leone, the virus led to 10%–16% of people admitted to hospitals every year (ACDC, 2018; Gonzalez, 2020; Newman, 2018; NICD, 2020; Richmond & Baglole, 2003). In 26 out of 36 Nigerian states, a case fatality ratio of 14.8% was recorded between January 1 to February 9, 2020 (WHO, 2020).

Several studies have laid a basis to understand the dynamics of Lassa fever. Some of the studies on Lassa Fever (Ojo et al., 2021; Onah et al., 2020; Onuorah et al., 2016) only considered the basic transmission pathways namely, the human-to-human and the rodent-to-human. Because a great percentage of people show little or no symptoms of Lassa fever, Peter, et al. (Peter et al., 2020) described Lassa fever transmission dynamics using a deterministic model integrating the exposed human and rat compartment instead of the usual SIR compartmental structure. Some other studies have tried to establish the time-dependent nature of the transmission dynamics of Lassa fever. For example, Ibrahim and Dénes (Ibrahim & Dénes, 2021) used a compartmental model with time-dependent parameters where the infectious class was partitioned into symptomatically infected, mildly infected and treated individuals alongside with the carrying capacity of the rodent because of the periodic change of weather. Factors like quarantine, hospitalization of infected individuals were also used in (Ibrahim & Dénes, 2021; Musa et al., 2020) to comprehend the transmission variability of Lassa fever. The association between the reproduction number and local rainfall was used to investigate the epidemiological features of Lassa fever on a large scale (Zhao et al., 2020). Abdulhamid et al. (Abdulhamid et al., 2022) incorporated the effect of quarantine and the environment to show that in poor resource countries, Lassa fever transmission is driven by environmental contribution. Differential infectivity has also been deployed as a technique to analyze the complex nature of Lassa fever dynamics (Musa et al., 2022). In order to understand the epidemiology of the disease, it is important to look at a number of possible transmission pathways through which the virus can be contracted. In this work, we focus on the effects of multiple transmission pathways of Lassa Fever towards the progression of the infection in the human and rodent population. The use of multiple transmission routes gives us a better understanding of the epidemiological structure of Lassa fever. Our study extends the work of Peter et al. (Peter et al., 2020) and Ibrahim and Dénes (Ibrahim & Dénes, 2021) by:

- Introducing the environment to human transmission pathway. We define the environment as the surfaces, walls and any other equipment where the virus is deposited.
- Introducing the aerosol to human route of transmission. By aerosol, we refer to air particles where the virus is concentrated through human and wind activities.

These two pathways are not usually considered as major drivers of infection on a large scale. In endemic areas like Nigeria, a major route of infection is the contact with infected rodents through harvesting, however, recent reports (Abdulhamid et al., 2022) have also shown that the environmental pathway contribute to the burden of Lassa fever and should not be neglected. Thus, our study captures (i) human to human transmission (ii) rodent to human transmission (iii) rodent to rodent

transmission (iv) environment to human transmission (v) aerosol to human transmission (vi) environment to rodent transmission. The aforementioned studies form the basic fabric for our work and the understanding gained from them will help us build and analyze a more comprehensive study with more transmission pathways. The remaining part of this work will be arranged thus: Section 2 will be the formulation of the basic model with basic analysis; In Section 3, we will perform our numerical simulations, and discussion and recommendations will be presented in Section 4.

2. Model formulation

The total human population, given as $N_H(t)$, is subdivided into five classes which consists of humans susceptible to the virus, $S_H(t)$, humans that have Lassa virus but are not infectious, $E_H(t)$, infectious humans that are asymptomatic, $I_{HA}(t)$, infectious humans that are symptomatic, $I_{HS}(t)$, and humans who have recovered from Lassa fever, $R_H(t)$ so that

$$N_H(t) = S_H(t) + E_H(t) + I_{HA}(t) + I_{HS}(t) + R_H(t). \tag{1}$$

The total rodent population, given as $N_R(t)$, is subdivided into three classes consisting of rodents susceptible to the virus, $S_R(t)$, rodents that have Lassa virus but are not infectious, $E_R(t)$, and infected rodents that can transmit the virus, $I_R(t)$ with

$$N_R(t) = S_R(t) + E_R(t) + I_R(t). \tag{2}$$

We consider the following direct transmission pathways: the human-to-human contact, the rodent-to-human contact, the rodent-to-rodent contact and the indirect transmission pathway such as the environment-to-human contact and the aerosol-to-human contact and the environment-to-rodent contact. To incorporate the indirect transmission pathways, we use V_S to describe the concentration of Lassa fever virus on the environmental surfaces and V_A, the concentration of Lassa virus in the air. The maximum carrying capacity of virus on environmental surfaces and in the air is given by K_V, where $V_S, V_A \leq K_V$.

We assume that π_1 is the constant recruitment rate of susceptible humans. The susceptible humans move to the exposed class, E_H, through a force of infection

$$\lambda_H = \beta_H \left(\frac{I_R}{N_R} + \frac{\eta_1 I_{HS}}{N_H} + \frac{\eta_2 I_{HA}}{N_H} + \frac{\eta_3 V_S}{K_V} + \frac{\eta_4 V_A}{K_V} \right). \tag{3}$$

Here, β_H is the effective contact rate between susceptible humans and infected rodents, susceptible humans and infectious humans, susceptible humans, the virus in the environment and the virus in the air, η_1 is the modification parameter which indicates that contact with I_{HS} is less infectious than with I_R. Similarly, η_2, η_3, η_4 are also modification parameters which account for level of infectiousness of contact with I_{HA}, V_S and V_A respectively. Evidence from (Bausch et al., 2010; Davies et al., 2019; Lehmann et al., 2017; Lo Iacono et al., 2015) ensures that the following inequality holds:

$$\eta_4 < \eta_3 < \eta_1 < \eta_2 < 1.$$

The exposed humans progress to the infectious compartment at the rate ψ_1, where the proportion of exposed individuals that become asymptomatic is $\nu\psi_1$ and the proportion of exposed persons that become symptomatic is $(1 - \nu)\psi_1$. Humans die naturally in all classes at the rate μ_1. Infectious symptomatic humans can die due to the disease at the rate δ but there are no cases of death due to infection for the infectious asymptomatic individuals. Infectious asymptomatic and infectious symptomatic humans recover at the rates ζ_1 and ζ_2, respectively.

The susceptible rodents are recruited at a constant rate π_2 and move to the exposed class E_R through a force of infection

$$\lambda_R = \beta_R \left(\frac{I_R}{N_R} + \frac{\xi_1 V_S}{K_V} \right), \tag{4}$$

where β_R is the effective contact rate between susceptible rodents and infected rodents and between susceptible rodents and contaminated environment surfaces. ξ_1 is the modification parameter which shows that contact with V_S is less infectious than with I_R. The exposed rodents move to the infectious class at the rate ψ_2 and all rodents die naturally at a rate of μ_2. Rodents can also die at a rate ρ due to consumption by humans as food. Rodents do not die due to disease since infected rodents can continue to shed the virus throughout their lifetime. The Lassa fever virus is deposited into the environment at rates of φ_1, φ_2 and φ_3 by infectious asymptomatic humans, infectious symptomatic humans, and infected rodents respectively through activities such as urination, excretion of faeces, bleeding and fluid secretions. We further assume that the virus concentration on the environmental surfaces and in the air decays at the rate θ_2 while a proportion of the virus concentration moves into the air at the rate θ_3 through wind and human activities.

The Lassa fever model in Fig. 1 is expressed as a system of first order nonlinear ordinary differential equations as follows:

$$\frac{dS_H}{dt} = \pi_1 - \lambda_H S_H - \mu_1 S_H,$$

$$\frac{dE_H}{dt} = \lambda_H S_H - (\psi_1 + \mu_1)E_H,$$

$$\frac{dI_{HA}}{dt} = \nu\psi_1 E_H - (\zeta_1 + \mu_1)I_{HA},$$

$$\frac{dI_{HS}}{dt} = (1 - \nu)\psi_1 E_H - (\delta + \zeta_2 + \mu_1)I_{HS},$$

$$\frac{dR_H}{dt} = \zeta_1 I_{HA} + \zeta_2 I_{HS} - \mu_1 R_H,$$

$$\frac{dS_R}{dt} = \pi_2 - \lambda_R S_R - (\rho + \mu_2)S_R,$$

$$\frac{dE_R}{dt} = \lambda_R S_R - (\psi_2 + \rho + \mu_2)E_R,$$

$$\frac{dI_R}{dt} = \psi_2 E_R - (\rho + \mu_2)I_R,$$

$$\frac{dV_S}{dt} = \varphi_1 I_{HA} + \varphi_2 I_{HS} + \varphi_3 I_R - (\theta_2 + \theta_3)V_S,$$

$$\frac{dV_A}{dt} = \theta_3 V_S - \theta_2 V_A,$$

$$(5)$$

which is subject to the following initial conditions:

$$
\begin{aligned}
S_H(0) &= S_{H_0} > 0, \quad E_H(0) = E_{H_0} \geq 0, \quad I_{HA}(0) = I_{HA_0} \geq 0, \\
I_{HS}(0) &= I_{HS_0} \geq 0, \quad R_H(0) = R_{H_0} \geq 0, \quad S_R(0) = S_{R_0} > 0, \\
E_R(0) &= E_{R_0} \geq 0, \quad I_R(0) = I_{R_0} \geq 0, \quad V_S(0) = V_{S_0} \geq 0, \\
V_A(0) &= V_{A_0} \geq 0, \quad \forall \ t \geq 0.
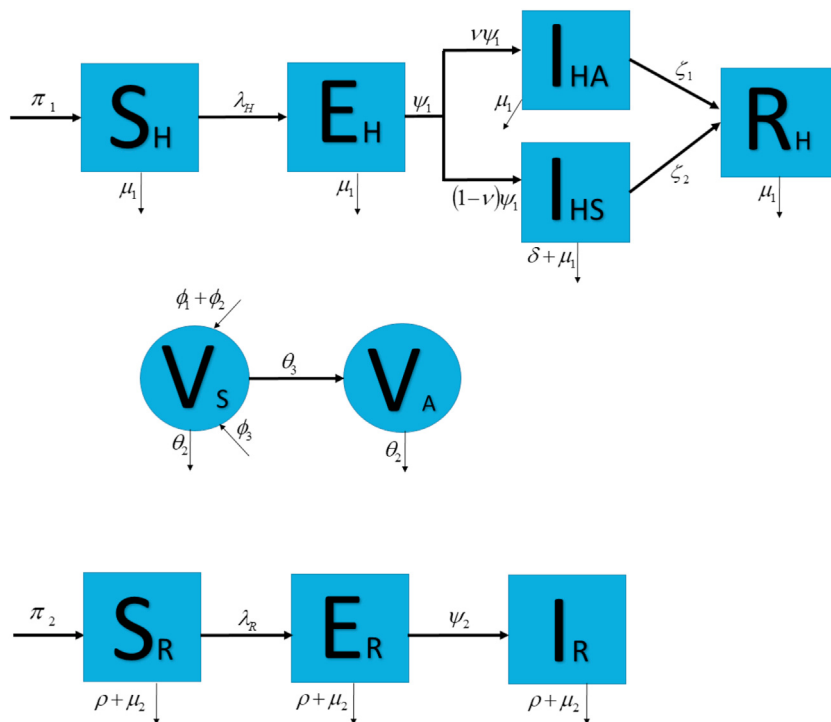\end{aligned}
$$

$$(6)$$

Fig. 1. The Lassa fever schematic diagram for human, virus and rodent population.

The variables and parameter descriptions and units are presented in Table 1.

2.1. Model analysis

Here, we show that our model is mathematically and biologically meaningful. We shall also compute the basic reproduction number and carry out the stability analysis of the steady states.

2.1.1. Feasible region

We assume that all parameters are non-negative for time t and prove that in the proposed region, Ω, the solutions remain non-negative and bounded. We will analyze the Lassa fever transmission model in the region given as:

$$\Omega = \left\{ \left(S_H, E_H, I_{HA}, I_{HS}, R_H, S_R, E_R, I_R, V_S, V_A \right) \in \Re_+^{10} : N_H \leq \frac{\pi_1}{\mu_1}, N_R \leq \frac{\pi_2}{\rho + \mu_2}, V_S \leq M_S, \ V_A \leq M_A \right\},$$

where

$$M_S = \frac{(\varphi_1 + \varphi_2)\pi_1}{\mu_1(\theta_2 + \theta_3)} + \frac{\varphi_3 \pi_2}{\mu_2(\theta_2 + \theta_3)}, \quad M_A = \frac{\theta_3 \pi_1 (\varphi_1 + \varphi_2)}{\mu_1 \theta_2 (\theta_2 + \theta_3)} + \frac{\theta_3 \varphi_3 \pi_2}{\mu_2 \theta_2 (\theta_2 + \theta_3)}.$$

To show that the region Ω is positively invariant, we consider the first equation of (5)

$$\frac{dS_H}{dt} = \pi_1 - (\lambda_H + \mu_1)S_H,$$

which is solved to obtain

Table 1
Description of parameters and variables for model (5).

Variables	Description	Unit
S_H	Susceptible human population	people
E_H	Exposed human population	people
I_{HA}	Infectious asymptomatic human population	people
I_{HS}	Infectious symptomatic human population	people
R_H	Recovered human population	people
S_R	Susceptible rodent population	rodents
E_R	Exposed rodent population	rodents
I_R	Infected rodent population	rodents
V_S	Concentration of Lassa virus in the environmental surfaces	virus
V_A	Concentration of Lassa virus in the air	virus
Parameters	**Description**	**Unit**
β_H	Contact rate between S_H and $I_R, I_{HA}, I_{HS}, V_S, V_A$	day^{-1}
η_1	Modification parameter	nil
η_2	Modification parameter	nil
η_3	Modification parameter	nil
η_4	Modification parameter	nil
β_R	Contact rate between S_R and I_R, V_S	day^{-1}
ξ_1	Modification parameter	nil
ψ_1	Rate of progression of humans from E_H to I_{HA} and I_{HS}	day^{-1}
ψ_2	Rate of progression of rodents from E_R to I_R	day^{-1}
θ_2	Rate of decay of virus in V_S	day^{-1}
θ_3	Rate of progression of virus from V_S to V_A	day^{-1}
φ_1	Rate at which virus is shed in V_S by I_{HA}	virus/people × day
φ_2	Rate at which virus is shed in V_S by I_{HS}	virus/people × day
φ_3	Rate at which virus is shed in V_S by I_R	virus/rodents × day
μ_1	Natural death rate of humans	day^{-1}
μ_2	Natural death rate of rodents	day^{-1}
ρ	Death rate of rodents due to consumption by humans	day^{-1}
ζ_1	Recovery rate of I_{HA}	day^{-1}
ζ_2	Recovery rate of I_{HS}	day^{-1}
π_1	Recruitment rate of humans	people/day
π_2	Recruitment rate of rodents	rodents/day
K_V	Maximum carrying capacity of virus	virus
δ	Disease-induced death rate of humans	day^{-1}
ν	Proportion of humans progressing to I_{HA}	nil

$$S_H(t) = S_{H_0} e^{-\int_0^t (\mu_1 + \lambda_H(s))ds} + \left[\frac{\pi_1}{\mu_1} e^{-\int_0^t (\mu_1 + \lambda_H(s))ds} \times \int_0^t e^{\int_0^s (\mu_1 + \lambda_H(r))dr} ds\right] > 0.$$

Also, for the solution component of $E_H(t)$, we suppose that there exist a first time t_1 such that $E_H(t_1) = 0$, $E'_H(t_1) < 0$ and the rest of the variables are non-negative for $0 < t_1 < t$. The second equation of system (5) gives

$$\frac{dE_H}{dt}\Big|_{t=t_1} = \lambda_H(t_1)S_H(t_1) > 0,$$

which is a contradiction, so $E_H(t) \geq 0$, $\forall\ t \geq 0$.

Using a similar approach, it is easy to show that $I_{HA}, I_{HS}, R_H, S_R, E_R, I_R, V_S, V_A$ are non-negative. Hence, all solutions of (5) are non-negative in Ω.

Now, we show that all solutions with non-negative initial conditions are bounded in the set Ω. It is easy to see that

$$\frac{dN_H}{dt} \leq \pi_1 - \mu_1 N_H, \quad \frac{dN_R}{dt} = \pi_2 - (\rho + \mu_2)N_R. \tag{6}$$

Solving the differential inequality and equation in (6), we use the standard comparison theorem (Lakshmikantham et al., 1989) and the integrating factor to show that as $t \to \infty$, we have that $0 \leq N_H(t) \leq \frac{\pi_1}{\mu_1}$ and $0 \leq N_R(t) = \frac{\pi_2}{\rho+\mu_2}$. Similarly the differential inequalities

$$\frac{dV_S}{dt} \leq (\varphi_1 + \varphi_2)\frac{\pi_1}{\mu_1} + \varphi_3 \frac{\pi_2}{\mu_2} - (\theta_2 + \theta_3)V_S, \quad \frac{dV_A}{dt} \leq \frac{\theta_3 \pi_1 (\varphi_1 + \varphi_2)}{\mu_1 \theta_2} + \frac{\theta_3 \varphi_3 \pi_2}{\mu_2 \theta_2} - \theta_2 V_A,$$

yield $V_S \leq \frac{(\varphi_1 + \varphi_2)\pi_1}{\mu_1(\theta_2 + \theta_3)} + \frac{\varphi_3 \pi_2}{\mu_2(\theta_2 + \theta_3)} = M_S$, $\quad V_A \leq \frac{\theta_3 \pi_1(\varphi_1 + \varphi_2)}{\mu_1 \theta_2(\theta_2 + \theta_3)} + \frac{\theta_3 \varphi_3 \pi_2}{\mu_2 \theta_2(\theta_2 + \theta_3)} = M_A$.

Thus, all possible solutions of (5) enter the region Ω and stay inside it. Hence, the region Ω is positively invariant and attracting and therefore a feasible region.

2.1.2. Reproduction number and equilibria stability analysis

We explore the existence of the equilibrium points of model (5). To obtain the disease free equilibrium (DFE), we equate the right hand side of model (5) to zero and solve when $E_H = I_{HA} = I_{HS} = E_R = I_R = V_S = V_A = 0$ to get:

$$E^0 = \left(\frac{\pi_1}{\mu_1}, 0, 0, 0, 0, \frac{\pi_2}{\rho + \mu_2}, 0, 0, 0, 0\right).$$

The basic reproduction number R_0 of model (5) is the dominant eigenvalue of the matrix FV^{-1} using the next generation matrix approach (Van den Driessche & Watmough, 2002). Here,

$$\mathcal{F} = \begin{pmatrix} \lambda_H S_H \\ 0 \\ 0 \\ \lambda_R S_R \\ 0 \\ 0 \\ 0 \end{pmatrix}, \quad \mathcal{V} = \begin{pmatrix} (\psi_1 + \mu_1)E_H \\ -\nu\psi_1 E_H + (\zeta_1 + \mu_1)I_{HA} \\ -(1-\nu)\psi_1 E_H + (\delta + \zeta_2 + \mu_1)I_{HS} \\ (\psi_2 + \rho + \mu_2)E_R \\ -\psi_2 E_R + (\rho + \mu_2)I_R \\ -\varphi_1 I_{HA} - \varphi_2 I_{HS} - \varphi_3 I_R + (\theta_2 + \theta_3)V_S \\ -\theta_3 V_S + \theta_2 V_A \end{pmatrix}.$$

Computing the Jacobian of $\mathcal{F}$ and $\mathcal{V}$ evaluated at E^0 we get

$$F = \begin{pmatrix} 0 & \beta_H \eta_2 & \beta_H \eta_1 & 0 & \dfrac{\beta_H \mu_2 \pi_1}{\mu_1 \pi_2} & \dfrac{\beta_H \eta_3 \pi_1}{\mu_1 K_V} & \dfrac{\beta_H \eta_4 \pi_1}{\mu_1 K_V} \\ 0 & 0 & 0 & 0 & 0 & 0 & 0 \\ 0 & 0 & 0 & 0 & 0 & 0 & 0 \\ 0 & 0 & 0 & 0 & \beta_R & \dfrac{\beta_R \xi_1 \pi_2}{\mu_2 K_V} & 0 \\ 0 & 0 & 0 & 0 & 0 & 0 & 0 \\ 0 & 0 & 0 & 0 & 0 & 0 & 0 \\ 0 & 0 & 0 & 0 & 0 & 0 & 0 \end{pmatrix},$$

$$V = \begin{pmatrix} \psi_1 + \mu_1 & 0 & 0 & 0 & 0 & 0 & 0 \\ -\nu\psi_1 & \zeta_1 + \mu_1 & 0 & 0 & 0 & 0 & 0 \\ -(1-\nu)\psi_1 & 0 & \delta + \zeta_2 + \mu_1 & 0 & 0 & 0 & 0 \\ 0 & 0 & 0 & \psi_2 + \rho + \mu_2 & 0 & 0 & 0 \\ 0 & 0 & 0 & -\psi_2 & \rho + \mu_2 & 0 & 0 \\ 0 & -\varphi_1 & -\varphi_2 & 0 & -\varphi_3 & (\theta_2 + \theta_3) & 0 \\ 0 & 0 & 0 & 0 & 0 & -\theta_3 & \theta_2 \end{pmatrix}.$$

The inverse of V is given as

$$V^{-1} = \begin{pmatrix} \dfrac{1}{\mu_1 + \psi_1} & 0 & 0 & 0 & 0 & 0 & 0 \\[2mm] \dfrac{\nu\psi_1}{(\zeta_1+\mu_1)(\mu_1+\psi_1)} & \dfrac{1}{\zeta_1+\mu_1} & 0 & 0 & 0 & 0 & 0 \\[2mm] -\dfrac{(-1+\nu)\psi_1}{(\delta+\zeta_2+\mu_1)(\mu_1+\psi_1)} & 0 & \dfrac{1}{\delta+\zeta_2+\mu_1} & 0 & 0 & 0 & 0 \\[2mm] 0 & 0 & 0 & \dfrac{1}{\mu_2+\rho+\psi_2} & 0 & 0 & 0 \\[2mm] 0 & 0 & 0 & \dfrac{\psi_2}{(\rho+\psi_2)(\mu_2+\rho+\psi_2)} & \dfrac{1}{\rho+\psi_2} & 0 & 0 \\[2mm] v_{61} & \dfrac{\varphi_1}{(\theta_2+\theta_3)(\zeta_1+\mu_1)} & v_{63} & v_{64} & \dfrac{\varphi_3}{(\theta_2+\theta_3)(\rho+\psi_2)} & \dfrac{1}{(\theta_2+\theta_3)} & 0 \\[2mm] v_{71} & \dfrac{\theta_3\varphi_1}{\theta_2(\theta_2+\theta_3)(\zeta_1+\mu_1)} & v_{73} & v_{74} & \dfrac{\theta_3\varphi_3}{\theta_2(\theta_2+\theta_3)(\rho+\psi_2)} & \dfrac{\theta_3}{\theta_2(\theta_2+\theta_3)} & \dfrac{1}{\theta_2} \end{pmatrix}$$

where

$$\begin{aligned} v_{61} &= -\frac{-((\delta+\zeta_2+\mu_1)\nu\psi_1\varphi_1) + (-1+\nu)(\zeta_1+\mu_1)\varphi_2\psi_1}{(\theta_2+\theta_3)(\zeta_1+\mu_1)(\delta+\zeta_2+\mu_1)(\mu_1+\psi_1)}, \\[2mm] v_{63} &= \frac{\varphi_2}{(\theta_2+\theta_3)(\delta+\zeta_2+\mu_1)}, \\[2mm] v_{64} &= \frac{\varphi_3\psi_2}{(\theta_2+\theta_3)(\rho+\psi_2)(\mu_2+\rho+\psi_2)}, \\[2mm] v_{71} &= -\frac{\theta_3(-((\delta+\zeta_2+\mu_1)\nu\psi_1\varphi_1) + (-1+\nu)(\zeta_1+\mu_1)\varphi_2\psi_1)}{\theta_2(\theta_2+\theta_3)(\zeta_1+\mu_1)(\delta+\zeta_2+\mu_1)(\mu_1+\psi_1)}, \\[2mm] v_{73} &= \frac{\theta_3\varphi_2}{\theta_2(\theta_2+\theta_3)(\delta+\zeta_2+\mu_1)}, \\[2mm] v_{74} &= \frac{\theta_3\varphi_3\psi_2}{\theta_2(\theta_2+\theta_3)(\rho+\psi_2)(\mu_2+\rho+\psi_2)}. \end{aligned}$$

(7a)

The next generation matrix evaluated at DFE is

$$FV^{-1} = \begin{pmatrix} b_{11} & b_{12} & b_{13} & b_{14} & b_{15} & b_{16} & b_{17} \\ 0 & 0 & 0 & 0 & 0 & 0 & 0 \\ 0 & 0 & 0 & 0 & 0 & 0 & 0 \\ b_{41} & b_{42} & b_{43} & b_{44} & b_{45} & b_{46} & 0 \\ 0 & 0 & 0 & 0 & 0 & 0 & 0 \\ 0 & 0 & 0 & 0 & 0 & 0 & 0 \\ 0 & 0 & 0 & 0 & 0 & 0 & 0 \end{pmatrix},$$

where

$$
\begin{aligned}
b_{11} &= \frac{\beta_H(K_V\theta_2(\theta_2+\theta_3)\mu_1(\eta_2(\delta+\zeta_2+\mu_1)\nu\psi_1 + (1-\nu)\eta_1(\zeta_1+\mu_1)\psi_1)}{K_V\theta_2(\theta_2+\theta_3)\mu_1(\zeta_1+\mu_1)(\delta+\zeta_2+\mu_1)(\mu_1+\psi_1)} \\
&\quad + \frac{\beta_H(\pi_1(\eta_3\theta_2+\eta_4\theta_3)((\delta+\zeta_2+\mu_1)\nu\psi_1\varphi_1 + (1-\nu)(\zeta_1+\mu_1)\varphi_2\psi_1)))}{K_V\theta_2(\theta_2+\theta_3)\mu_1(\zeta_1+\mu_1)(\delta+\zeta_2+\mu_1)(\mu_1+\psi_1)}, \\
b_{12} &= \frac{\beta_H\eta_2}{(\zeta_1+\mu_1)} + \frac{\pi_1\beta_H\eta_3\varphi_1}{K_V(\theta_2+\theta_3)\mu_1(\zeta_1+\mu_1)} + \frac{\pi_1\beta_H\eta_4\theta_3\varphi_1}{K_V\theta_2(\theta_2+\theta_3)\mu_1(\zeta_1+\mu_1)}, \\
b_{13} &= \frac{\beta_H\eta_1}{(\delta+\zeta_2+\mu_1)} + \frac{\pi_1\beta_H\eta_3\varphi_2}{K_V(\theta_2+\theta_3)\mu_1(\delta+\zeta_2+\mu_1)} + \frac{\pi_1\beta_H\eta_4\theta_3\varphi_2}{K_V\theta_2(\theta_2+\theta_3)\mu_1(\delta+\zeta_2+\mu_1)}, \\
b_{14} &= \frac{\pi_1\beta_H(K_V\theta_2(\theta_2+\theta_3)\mu_2 + \pi_2(\eta_3\theta_2+\eta_4\theta_3)\varphi_3)\psi_2}{K_V\pi_2\theta_2(\theta_2+\theta_3)\mu_1(\rho+\psi_2)(\mu_2+\rho+\psi_2)}, \\
b_{15} &= \frac{\pi_1\beta_H\mu_2}{\pi_2\mu_1(\rho+\psi_2)} + \frac{\pi_1\beta_H\eta_3\varphi_3}{K_V(\theta_2+\theta_3)\mu_1(\rho+\psi_2)} + \frac{\pi_1\beta_H\eta_4\theta_3\varphi_3}{K_V\theta_2(\theta_2+\theta_3)\mu_1(\rho+\psi_2)}, \\
b_{16} &= \frac{\pi_1\beta_H\eta_3}{K_V(\theta_2+\theta_3)\mu_1} + \frac{\pi_1\beta_H\eta_4\theta_3}{K_V\theta_2(\theta_2+\theta_3)\mu_1}, \quad b_{17} = \frac{\pi_1\beta_H\eta_4}{K_V\theta_2\mu_1}, \\
b_{41} &= \frac{\pi_2\beta_R\xi_1((\delta+\zeta_2+\mu_1)\nu\psi_1\varphi_1 + (1-\nu)(\zeta_1+\mu_1)\varphi_2\psi_1)}{K_V(\theta_2+\theta_3)(\zeta_1+\mu_1)(\delta+\zeta_2+\mu_1)\mu_2(\mu_1+\psi_1)}, \\
b_{42} &= \frac{\pi_2\beta_R\xi_1\varphi_1}{K_V(\theta_2+\theta_3)(\zeta_1+\mu_1)\mu_2}, \quad b_{43} = \frac{\pi_2\beta_R\xi_1\varphi_2}{K_V(\theta_2+\theta_3)(\delta+\zeta_2+\mu_1)\mu_2}, \\
b_{44} &= \frac{\beta_R(K_V(\theta_2+\theta_3)\mu_2 + \pi_2\xi_1\varphi_3)\psi_2}{K_V(\theta_2+\theta_3)\mu_2(\rho+\psi_2)(\mu_2+\rho+\psi_2)}, \\
b_{45} &= \frac{\beta_R}{(\rho+\psi_2)} + \frac{\pi_2\beta_R\xi_1\varphi_3}{K_V(\theta_2+\theta_3)\mu_2(\rho+\psi_2)}, \quad b_{46} = \frac{\pi_2\beta_R\xi_1}{K_V(\theta_2+\theta_3)\mu_2}.
\end{aligned}
$$
(7b)

The basic reproduction number is given by

$$R_0 = \frac{b_{11}+b_{44}}{2} + \frac{\sqrt{(b_{11}-b_{44})^2 + 4b_{14}b_{41}}}{2}.$$
(7c)

Remark 2.1.1. (i) The terms contained in R_0 represent the direct and indirect transmission pathways. They are described thus: b_{11} is the local reproduction number of infectious asymptomatic humans, infectious symptomatic humans, contaminated environmental surfaces and contaminated air particles in the progression of Lassa Fever virus in the human population only; b_{44} is the local reproduction number of infected rodents and contaminated environmental surfaces in the progression of Lassa Fever virus in the rodent population only; b_{14} is the local reproduction number of contaminated environmental surfaces and contaminated air particles in the progression of Lassa Fever virus in the human population only; and b_{41} is the local reproduction number of contaminated environmental surfaces in the progression of Lassa Fever virus in the rodent population only.

(ii) It is easy to see that

$$(b_{11} - b_{44})^2 + 4b_{14}b_{41} = (b_{11} + b_{44})^2 + 4(b_{14}b_{41} - b_{11}b_{44}).$$

Thus, $b_{14}b_{41} > b_{11}b_{44}$ implies that $R_0 > 0$. This condition ensures that infection will be sustained across from rodents to humans and from humans to rodents via all the transmission pathways.

(iii) The local stability of the disease free equilibrium point when $R_0 < 1$ is ensured by the hypothesis used in the computation of R_0 (Van den Driessche & Watmough, 2002).

Theorem 2.1.1. *The disease free equilibrium point is globally asymptotically stable if $R_0 < 1$.*

Proof. It suffices to show that our model (5) satisfy conditions **H1** and **H2** of the global stability theorem by (Castillo-Chavez et al., 2002) when $R_0 < 1$.

Model (5) can be rewritten in the form

$$\frac{dX}{dt} = F(X, Y),$$

$$\frac{dY}{dt} = G(X, Y), \quad G(X, \mathbf{0}) = 0.$$

Here, $X = (S_H, S_R)^T$, $Y = (E_H, I_{HA}, I_{HS}, E_R, I_R, V_S, V_A)^T$, $X \in \Re^2_+$ represents the number of susceptible humans and rodents and $Y \in \Re^7_+$ represents the number of exposed humans, asymptomatic infectious humans, symptomatic infectious humans, exposed rodents, infected rodents, contaminated environment and contaminated air.

Our DFE is now written as $E_0 = (X, \mathbf{0})$ where $X_0 = (\frac{\pi_1}{\mu_1}, \frac{\pi_2}{\rho + \mu_2})$ and we show that the following conditions are satisfied:

- **H1**: For $\frac{dX}{dt} = F(X_0, \mathbf{0})$, X_0 is globally asymptotically stable.
- **H2**: $G(X, Y) = AY - \hat{G}(X, Y), \hat{G}(X, Y) \geq 0$ for $(X, Y) \in \Omega$ where $A = D_Y(G(X_0, \mathbf{0}))$ is an M-matrix and Ω is the region where the model makes biological sense.

For the first condition **H1**, we have

$$\frac{dS_H}{dt} = \pi_1 - \mu_1 S_H, \quad \frac{dS_R}{dt} = \pi_2 - (\rho + \mu_2)S_R, \tag{8}$$

which can be solved to get

$$S_H(t) = \frac{\pi_1}{\mu_1} + \left(\frac{\pi_1}{\mu_1} - S_{H_0}\right)e^{-\mu_1 t}, \quad S_R(t) = \frac{\pi_2}{\rho + \mu_2} + \left(\frac{\pi_2}{\rho + \mu_2} - S_{R_0}\right)e^{-(\rho + \mu_2)t}.$$

We take limits as $t \to \infty$ to get,

$$\lim_{t \to \infty} S_H(t) = \frac{\pi_1}{\mu_1}, \quad \lim_{t \to \infty} S_R(t) = \frac{\pi_2}{\rho + \mu_2}.$$

Hence, the solutions of equation (8) converge to X_0 regardless of the initial conditions. Therefore, X_0 is a globally asymptotically equilibrium point of (8).

For condition **H2**, we consider $F(X, 0) = (\pi_1 - \mu_1 S_H, \pi_2 - (\rho + \mu_2)S_R)$, $G(X, Y) = AY - \hat{G}(X, Y)$
where

$$G(X,Y) = \begin{pmatrix} \lambda_H S_H - (\psi_1 + \mu_1)E_H \\ \nu\psi_1 E_H - (\zeta_1 + \mu_1)I_{HA} \\ (1-\nu)\psi_1 E_H - (\delta + \zeta_2 + \mu_1)I_{HS} \\ \lambda_R S_R - (\psi_2 + \rho + \mu_2)E_R \\ \psi_2 E_R - (\rho + \mu_2)I_R \\ \varphi_1 I_{HA} + \varphi_2 I_{HS} + \varphi_3 I_R - (\theta_2 + \theta_3)V_S \\ \theta_3 V_S - \theta_2 V_A \end{pmatrix},$$

and

$$A = \begin{pmatrix} -(\psi_1+\mu_1) & \beta_H\eta_2 & \beta_H\eta_1 & 0 & \dfrac{\beta_H\mu_2\pi_1}{\mu_1\pi_2} & \dfrac{\beta_H\eta_3\pi_1}{\mu_1 K_V} & \dfrac{\beta_H\eta_4\pi_1}{\mu_1 K_V} \\ \nu\psi_1 & -(\zeta_1+\mu_1) & 0 & 0 & 0 & 0 & 0 \\ (1-\nu)\psi_1 & 0 & -(\delta+\zeta_2+\mu_1) & 0 & 0 & 0 & 0 \\ 0 & 0 & 0 & -(\psi_2+\rho+\mu_2) & \beta_R & \dfrac{\beta_R\xi_1\pi_2}{\mu_2 K_V} & 0 \\ 0 & 0 & 0 & \psi_2 & -(\rho+\mu_2) & 0 & 0 \\ 0 & \varphi_1 & \varphi_2 & 0 & \varphi_3 & -(\theta_2+\theta_3) & 0 \\ 0 & 0 & 0 & 0 & 0 & \theta_3 & -\theta_2 \end{pmatrix},$$

which is an M-matrix and

$$\hat{G}(X,Y) = \begin{pmatrix} \beta_H\eta_2(S_H^0 - S_H) + \beta_H\eta_1(S_H^0 - S_H) + \dfrac{\beta_H\mu_2}{\pi_2}(S_H^0 - S_H) + \dfrac{\beta_H\eta_3}{K_V}(S_H^0 - S_H) + \dfrac{\beta_H\eta_4}{K_V}(S_H^0 - S_H) \\ 0 \\ 0 \\ \beta_R(S_R^0 - S_R) + \dfrac{\beta_R\xi_1}{K_V}(S_R^0 - S_R) \\ 0 \\ 0 \\ 0 \end{pmatrix}.$$

Clearly, $\hat{G}(X,Y) \geq 0$ since $0 \leq S_H \leq S_H^0$ and $0 \leq S_R \leq S_R^0$. $\square$

The global stability of E^0 thus follows and the Lassa fever virus can be eliminated from the human and rodent population over a period of time provided $R_0 < 1$.

The endemic equilibrium point of the model (5) is given by

$$E^* = (S_H^*, E_H^*, I_{HA}^*, I_{HS}^*, R_H^*, S_R^*, E_R^*, I_R^*, V_S^*, V_A^*),$$

where

$$S_H^* = \frac{\pi_1}{\lambda_H^* + \mu_1}, \quad E_H^* = \frac{\pi_1\lambda_H^*}{(\psi_1 + \mu_1)(\lambda_H^* + \mu_1)}, \quad I_{HA}^* = \frac{\nu\psi_1\pi_1\lambda_H^*}{(\zeta_1 + \mu_1)(\psi_1 + \mu_1)(\lambda_H^* + \mu_1)},$$

$$I_{HS}^* = \frac{(1-\nu)\psi_1\pi_1\lambda_H^*}{(\delta + \zeta_2 + \mu_1)(\psi_1 + \mu_1)(\lambda_H^* + \mu_1)},$$

$$R_H^* = \frac{\zeta_1\nu\psi_1\pi_1\lambda_H^*}{\mu_1(\zeta_1 + \mu_1)(\psi_1 + \mu_1)(\lambda_H^* + \mu_1)} + \frac{\zeta_2(1-\nu)\psi_1\pi_1\lambda_H^*}{\mu_1(\delta + \zeta_2 + \mu_1)(\psi_1 + \mu_1)(\lambda_H^* + \mu_1)},$$

$$S_R^* = \frac{\pi_2}{\lambda_R^* + \rho + \mu_2}, \quad E_R^* = \frac{\pi_2\lambda_R^*}{(\psi_2 + \rho + \mu_2)(\lambda_R^* + \rho + \mu_2)}, \quad I_R^* = \frac{\psi_2\pi_2\lambda_R^*}{(\rho + \mu_2)(\psi_2 + \rho + \mu_2)(\lambda_R^* + \rho + \mu_2)},$$

$$V_S^* = \frac{\varphi_1\nu\psi_1\pi_1\lambda_H^*}{(\theta_2 + \theta_3)(\zeta_1 + \mu_1)(\psi_1 + \mu_1)(\lambda_H^* + \mu_1)} + \frac{\varphi_2(1-\nu)\psi_1\pi_1\lambda_H^*}{(\theta_2 + \theta_3)(\delta + \zeta_2 + \mu_1)(\psi_1 + \mu_1)(\lambda_H^* + \mu_1)}$$

$$+ \frac{\varphi_3\psi_2\pi_2\lambda_R^*}{(\theta_2 + \theta_3)(\rho + \mu_2)(\psi_2 + \rho + \mu_2)(\lambda_R^* + \rho + \mu_2)},$$

$$V_A^* = \frac{\theta_3\varphi_1\nu\psi_1\pi_1\lambda_H^*}{\theta_2(\theta_2 + \theta_3)(\zeta_1 + \mu_1)(\psi_1 + \mu_1)(\lambda_H^* + \mu_1)} + \frac{\theta_3\varphi_2(1-\nu)\psi_1\pi_1\lambda_H^*}{\theta_2(\theta_2 + \theta_3)(\delta + \zeta_2 + \mu_1)(\psi_1 + \mu_1)(\lambda_H^* + \mu_1)}$$

$$+ \frac{\theta_3\varphi_3\psi_2\pi_2\lambda_R^*}{\theta_2(\theta_2 + \theta_3)(\rho + \mu_2)(\psi_2 + \rho + \mu_2)(\lambda_R^* + \rho + \mu_2)},$$

(9)

and

$$\lambda_H^* = \beta_H\left(\frac{I_R^*}{N_R^*} + \frac{\eta_1 I_{HS}^*}{N_H^*} + \frac{\eta_2 I_{HA}^*}{N_H^*} + \frac{\eta_3 V_S^*}{K_V^*} + \frac{\eta_4 V_A^*}{K_V^*}\right), \tag{9}$$

$$\lambda_R^* = \beta_R\left(\frac{I_R^*}{N_R^*} + \frac{\xi_1 V_S^*}{K_V^*}\right). \tag{10}$$

Equations (9) and (10) can be written explicitly as

$$\lambda_H^* = \frac{\mu_1 b_{11}\lambda_H^*}{(\lambda_H^* + \mu_1)} + \frac{\mu_1\pi_2 b_{14}\lambda_R^*}{\pi_1(\lambda_R^* + \rho + \mu_2)}, \tag{11}$$

$$\lambda_R^* = \frac{\mu_2\pi_1 b_{41}\lambda_H^*}{\pi_2(\lambda_H^* + \mu_1)} + \frac{\mu_2 b_{44}\lambda_R^*}{(\lambda_R^* + \rho + \mu_2)}. \tag{12}$$

We see that the state variables are expressed in terms of λ_H^* and λ_R^*. From here, we proceed by using the approach in (Moghadas et al., 2003; Velasco-Hernandez & Hsieh, 1994). Hence, we can obtain positive equilibrium points of the model by finding the fixed points of equations (11) and (12) as

$$c(\lambda_H, \lambda_R) = \begin{pmatrix} c_1(\lambda_H, \lambda_R) \\ c_2(\lambda_H, \lambda_R) \end{pmatrix},$$

where

$$\begin{pmatrix} c_1(\lambda_H, \lambda_R) \\ c_2(\lambda_H, \lambda_R) \end{pmatrix}$$

corresponds to the right hand sides of equations (11) and (12).

Theorem 2.1.2. *There exists a unique fixed point* $(\lambda_H^*, \lambda_R^*)$, $\lambda_H^* > 0$, $\lambda_R^* > 0$ *which satisfies*

$$c(\lambda_H^*, \lambda_R^*) = \begin{pmatrix} c_1(\lambda_H^*, \lambda_R^*) \\ c_2(\lambda_H^*, \lambda_R^*) \end{pmatrix}$$

and corresponds to the endemic equilibrium point E^* (Moghadas et al., 2003; Velasco-Hernandez & Hsieh, 1994).

Proof. From the first equation, we fix $\lambda_R > 0$ and look at the real-valued function depending on λ_H:

$$c_1^{\lambda_R}(\lambda_H) = \frac{\mu_1 b_{11} \lambda_H}{(\lambda_H + \mu_1)} + \frac{\mu_1 \pi_2 b_{14} \lambda_R}{\pi_1 (\lambda_R + \rho + \mu_2)}.$$

We have that

$$\lim_{\lambda_H \to 0} c_1^{\lambda_R}(\lambda_H) = \frac{\mu_1 \pi_2 b_{14} \lambda_R}{\pi_1 (\lambda_R + \rho + \mu_2)} < \infty,$$

and

$$\lim_{\lambda_H \to \infty} c_1^{\lambda_R}(\lambda_H) = \mu_1 b_{11} + \frac{\mu_1 \pi_2 b_{14} \lambda_R}{\pi_1 (\lambda_R + \rho + \mu_2)} < \infty.$$

It follows that $0 < c_1^{\lambda_R}(\lambda_H) < \infty$ which implies that $c_1^{\lambda_R}(\lambda_H)$ is bounded for every fixed $\lambda_R > 0$.
Next,

$$\frac{\partial c_1^{\lambda_R}(\lambda_H)}{\partial \lambda_H} = \frac{\mu_1^2 b_{11}}{(\lambda_H + \mu_1)^2},$$

and

$$\frac{\partial^2 c_1^{\lambda_R}(\lambda_H)}{\partial^2 \lambda_H} = -\frac{2\mu_1^2 b_{11}}{(\lambda_H + \mu_1)^3}.$$

$c_1^{\lambda_R}(\lambda_H)$ is an increasing concave down function since $\frac{\partial c_1^{\lambda_R}(\lambda_H)}{\partial \lambda_H} > 0$ and $\frac{\partial^2 c_1^{\lambda_R}(\lambda_H)}{\partial^2 \lambda_H} < 0$. Hence, there is no change in concavity of c_1 in the bounded domain. It follows that there exists a unique $\lambda_H^* > 0$ which satisfies $c_1^{\lambda_R}(\lambda_H^*) = \lambda_H^*$.
For this $\lambda_H^* > 0$, we look at the real-valued function depending on λ_R:

$$c_2^{\lambda_H^*}(\lambda_R) = \frac{\mu_2 \pi_1 b_{41} \lambda_H^*}{\pi_2 (\lambda_H^* + \mu_1)} + \frac{\mu_2 b_{44} \lambda_R}{(\lambda_R + \rho + \mu_2)}.$$

Then,

$$\lim_{\lambda_R \to 0} c_2^{\lambda_H^*}(\lambda_R) = \frac{\mu_2 \pi_1 b_{41} \lambda_H^*}{\pi_2 (\lambda_H^* + \mu_1)} < \infty,$$

and

$$\lim_{\lambda_R \to \infty} c_2^{\lambda_H^*}(\lambda_R) = \mu_2 b_{44} + \frac{\mu_2 \pi_1 b_{41} \lambda_H^*}{\pi_2 (\lambda_H^* + \mu_1)} < \infty.$$

It follows that $0 < c_2^{\lambda_H^*}(\lambda_R) < \infty$ which implies that $c_2^{\lambda_H^*}(\lambda_R)$ is bounded for every fixed $\lambda_H^* > 0$.
Next,

$$\frac{\partial c_2^{\lambda_H^*}(\lambda_R)}{\partial \lambda_R} = \frac{\mu_2 b_{44}(\rho + \mu_2)}{(\lambda_R + \rho + \mu_2)^2},$$

and

$$\frac{\partial^2 c_2^{\lambda_H^*}(\lambda_R)}{\partial^2 \lambda_R} = -\frac{2\mu_2 b_{44}(\rho + \mu_2)}{(\lambda_R + \rho + \mu_2)^3}.$$

$c_2^{\lambda_H^*}(\lambda_R)$ is an increasing concave down function since $\frac{\partial c_2^{\lambda_H^*}(\lambda_R)}{\partial \lambda_R} > 0$ and $\frac{\partial^2 c_2^{\lambda_H^*}(\lambda_R)}{\partial^2 \lambda_R} < 0$. Hence, there is no change in the concavity of

c_2 in the positive domain. It follows that there exists a unique $\lambda_R^* > 0$ which satisfies $c_2^{\lambda_H^*}(\lambda_R^*) = \lambda_R^*$.

Therefore, there is a fixed point $(\lambda_H^*, \lambda_R^*)$ which corresponds to the endemic equilibrium point E^*. $\square$

We now investigate the stability of the equilibrium points using the stability of the fixed point system $(\lambda_H^*, \lambda_R^*)$ corresponding to E^*. The Jacobian of the system is given by:

$$J(\lambda_H^*, \lambda_R^*) = \begin{pmatrix} \dfrac{\partial c_1}{\partial \lambda_H^*} & \dfrac{\partial c_1}{\partial \lambda_R^*} \\[2ex] \dfrac{\partial c_2}{\partial \lambda_H^*} & \dfrac{\partial c_2}{\partial \lambda_R^*} \end{pmatrix}, \tag{13}$$

where

$$\frac{\partial c_1}{\partial \lambda_H^*} = \frac{\mu_1^2 b_{11}}{(\lambda_H + \mu_1)^2}, \quad \frac{\partial c_1}{\partial \lambda_R^*} = \frac{\mu_1 \pi_2 b_{14}(\rho + \mu_2)^2}{\pi_1 \mu_2 (\lambda_R + \rho + \mu_2)^2}, \quad \frac{\partial c_2}{\partial \lambda_H^*} = \frac{\mu_1 \mu_2 \pi_1 b_{41}}{\pi_2 (\lambda_H + \mu_1)^2}, \quad \frac{\partial c_2}{\partial \lambda_R^*} = \frac{b_{44}(\rho + \mu_2)^2}{(\lambda_R + \rho + \mu_2)^2}.$$

We note that $J(\lambda_H^*, \lambda_R^*)$ evaluated at the fixed point, $(\lambda_H^*, \lambda_R^*) = (0,0)$, is given by

$$J(0,0) = \begin{pmatrix} b_{11} & \dfrac{\mu_1 \pi_2 b_{14}}{\pi_1 \mu_2} \\[2ex] \dfrac{\mu_2 \pi_1 b_{41}}{\pi_2 \mu_1} & b_{44} \end{pmatrix},$$

and for stability, we require that $|\lambda_i| < 1$, where λ_i are the eigenvalues of $J(0, 0)$, which corresponds to

$$R_0 = \frac{b_{11} + b_{44}}{2} + \frac{\sqrt{(b_{11} - b_{44})^2 + 4b_{14}b_{41}}}{2} < 1. \tag{14}$$

Hence, the stability of $(\lambda_H^*, \lambda_R^*) = (0,0)$ is achieved when $R_0 < 1$. The point is unstable provided $R_0 > 1$. Thus, the stability of $(\lambda_H^*, \lambda_R^*) = (0,0)$ corresponds to the stability of E^0 when $R_0 < 1$. Now, for $(\lambda_H^*, \lambda_R^*) \neq (0,0)$, we have

$$J(\lambda_H^*, \lambda_R^*) = \begin{pmatrix} d_{11} & d_{12} \\ d_{21} & d_{22} \end{pmatrix},$$

and for stability, we require that $|\lambda_i| < 1$, that is,

$$\left| \frac{d_{11} + d_{22}}{2} + \frac{\sqrt{(d_{11} - d_{22})^2 + 4d_{12}d_{21}}}{2} \right| < 1,$$

where

$$d_{11} = \frac{\mu_1^2 b_{11}}{(\lambda_H^* + \mu_1)^2}, \quad d_{12} = \frac{\mu_1 \pi_2 b_{14}(\rho + \mu_2)^2}{\pi_1 \mu_2 (\lambda_R^* + \rho + \mu_2)^2}, \quad d_{21} = \frac{\mu_1 \mu_2 \pi_1 b_{41}}{\pi_2 (\lambda_H^* + \mu_1)^2}, \quad d_{22} = \frac{b_{44}(\rho + \mu_2)^2}{(\lambda_R^* + \rho + \mu_2)^2}.$$

The stability of the fixed point system is governed by the fact that the absolute value of the eigenvalues of the fixed point system is less than unity (Moghadas et al., 2003; Velasco-Hernandez & Hsieh, 1994). Hence, $|\lambda_i| < 1$ corresponds to

$$\frac{1 + d_{11}d_{22}}{d_{11} + d_{22} + d_{12}d_{21}} > 1. \tag{15}$$

Defining the left hand side of (15) as $R(\lambda_H^*, \lambda_R^*)$, the fixed point $(\lambda_H^*, \lambda_R^*) \neq (0,0)$ is stable when $R(\lambda_H^*, \lambda_R^*) > 1$.

2.1.3. Global stability of endemic equilibrium and bifurcation analysis

We first show that E^* is globally asymptotically stable using the following theorem:

Theorem 2.1.3. *The endemic equilibrium point E^* of model (5) is globally asymptotically stable when $\frac{\mu_2 \pi_1 b_{41}}{\pi_2 (c + \mu_1)} + \frac{\mu_2 b_{44}}{(c + \rho + \mu_2)} > 1$.*

Table 2
Parameter values and references.

Parameters	Value	Reference
π_1	0.497	Calculated
π_2	2.74	Calculated
μ_1	0.0000497	Trends (2021)
μ_2	0.00274	Control (2018)
ψ_1	0.0094	Assumed
ψ_2	0.048	Assumed
β_H	0.00017	Assumed
β_R	0.004	Assumed
ρ	0.0006	(Ossai et al., 2020; WHO, 2021)
ν	0.8	(CDC, 2014; WHO, 2017; Yun & Walker, 2012)
ζ_1	0.0000476	Estimated
ζ_2	0.0000323	Estimated
δ	0.0005	NCDC (2021)
θ_2	0.01868	Estimated
θ_3	0.00701	Stephenson et al. (1984)
φ_1	0.0667	Assumed
φ_2	0.0357	Assumed
φ_3	0.02569	Assumed
ξ_1	0.167	Assumed
η_1	0.94	Assumed
η_2	0.95	Assumed
η_3	0.9	Assumed
η_4	0.85	Assumed

Table 3
Sensitivity indices of R_0.

Parameters	Sensitivity indices of R_0	Parameters	Sensitivity indices of R_0
π_1	0.444782	δ	−0.0272335
π_2	0.0000581831	θ_2	−0.439338
μ_1	−0.946283	θ_3	−0.00550217
μ_2	−0.000168322	φ_1	0.43505
ψ_1	0.00524857	φ_2	0.00973221
ψ_2	−0.00190397	φ_3	0.0000581831
β_H	0.997936	ξ_1	0.00199971
β_R	0.0020637	η_1	0.0219675
ρ	−0.0000495958	η_2	0.531187
ν	0.839438	η_3	0.32696
ζ_1	−0.472691	η_4	0.115881
ζ_2	−0.00175928		

Proof. We use the geometric approach in (Li & Muldowney, 1996). Let us consider the fixed point system (11) and (12). We convert it to a root finding problem to get

$$
\begin{aligned}
\hat{f}_1 &= \frac{\mu_1 b_{11} \lambda_H^*}{(\lambda_H^* + \mu_1)} + \frac{\mu_1 \pi_2 b_{14} \lambda_R^*}{\pi_1 (\lambda_R^* + \rho + \mu_2)} - \lambda_H^*, \\
\hat{f}_2 &= \frac{\mu_2 \pi_1 b_{41} \lambda_H^*}{\pi_2 (\lambda_H^* + \mu_1)} + \frac{\mu_2 b_{44} \lambda_R^*}{(\lambda_R^* + \rho + \mu_2)} - \lambda_R^*.
\end{aligned}
\tag{16}
$$

The Jacobian matrix corresponding to this system is

$$
J = \begin{pmatrix} f_{11} - 1 & f_{12} \\ f_{21} & f_{22} - 1 \end{pmatrix},
$$

where

$$
f_{11} = \frac{\mu_1^2 b_{11}}{(\lambda_H + \mu_1)^2}, \quad f_{12} = \frac{\mu_1 \pi_2 b_{14}(\rho + \mu_2)}{\pi_1 (\lambda_R + \rho + \mu_2)^2}, \quad f_{21} = \frac{\mu_1 \mu_2 \pi_1 b_{41}}{\pi_2 (\lambda_H + \mu_1)^2}, \quad f_{22} = \frac{\mu_2 b_{44}(\rho + \mu_2)}{(\lambda_R + \rho + \mu_2)^2}.
$$

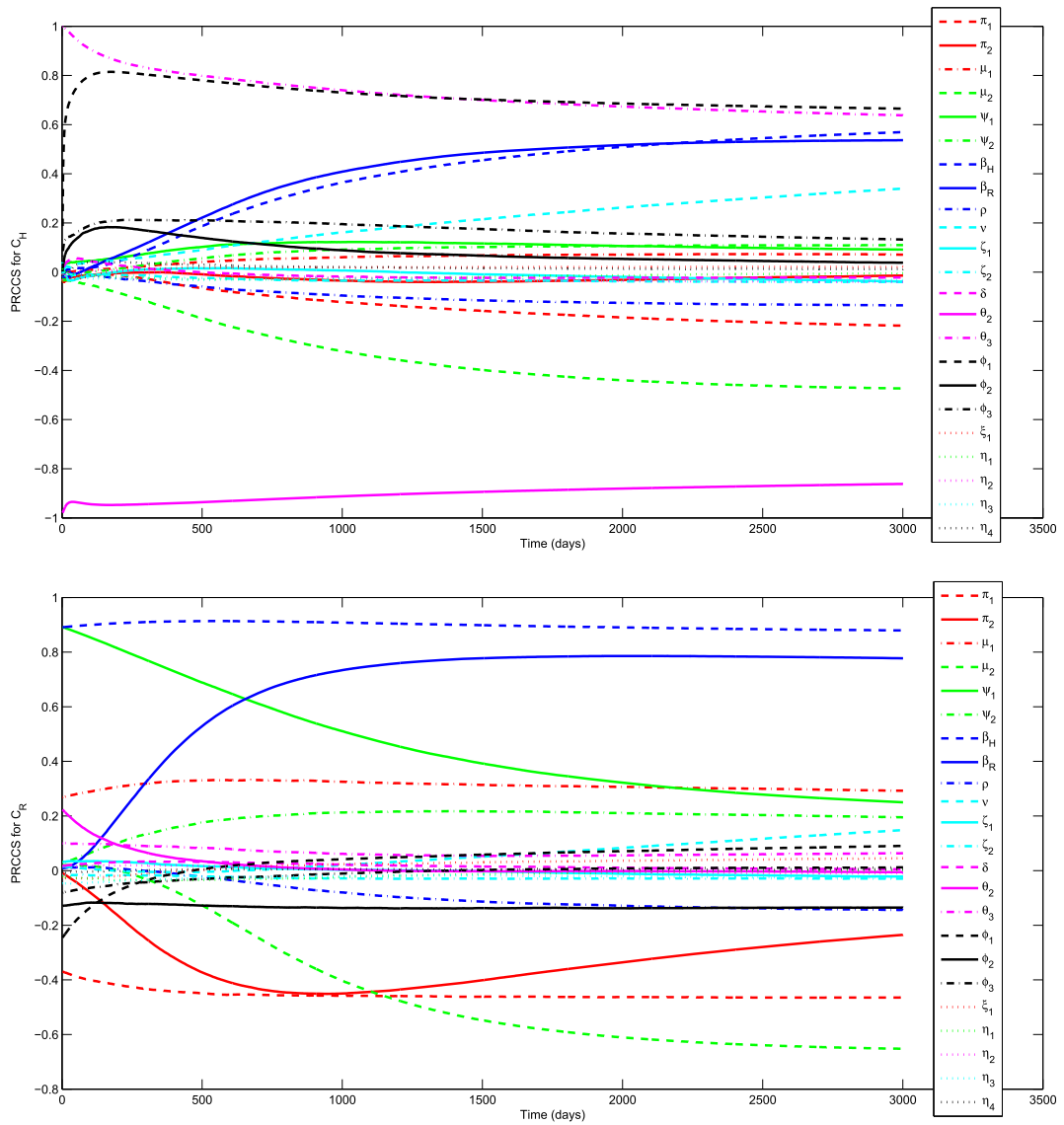The second additive compound matrix (Muldowney, 1990) of J is

Fig. 2. Partial Rank Correlation Coefficient for the full range of parameters of model (5) in the cumulative cases of human and rodent population.

$$J^{[2]} = \left[\frac{\mu_1^2 b_{11}}{(\lambda_H + \mu_1)^2} + \frac{\mu_2 b_{44}(\rho + \mu_2)}{(\lambda_R + \rho + \mu_2)^2} - 2 \right] \equiv [\mathcal{C}].$$

We assume the function

$$Q = Q(\lambda_H, \lambda_R) = \begin{bmatrix} \dfrac{\lambda_H}{\lambda_R} & 0 \\ 0 & \dfrac{\lambda_H}{\lambda_R} \end{bmatrix},$$
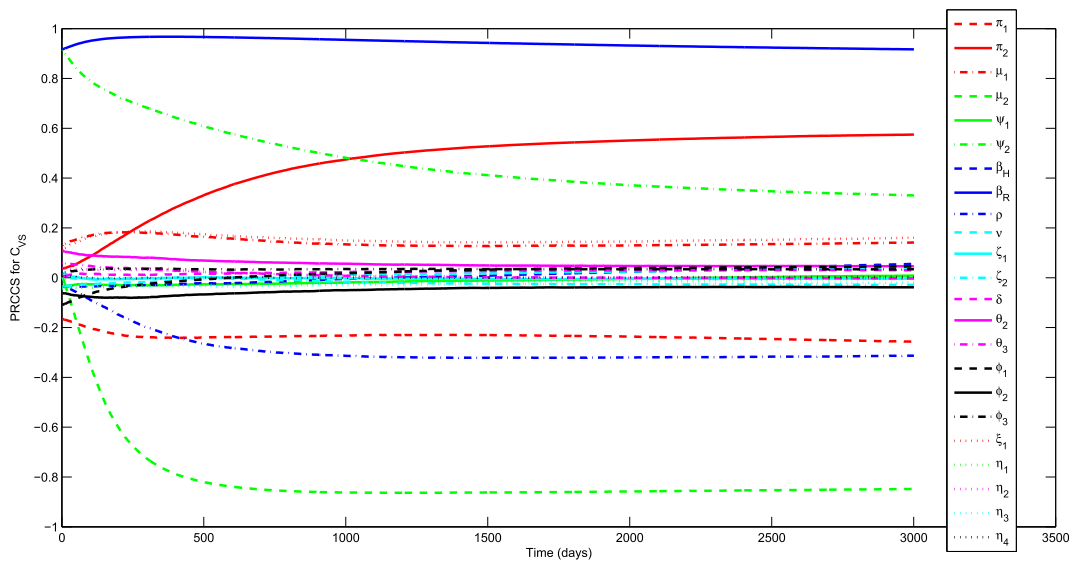
we have

Fig. 3. Partial Rank Correlation Coefficient for the full range of parameters of model (5) in the cumulative cases of virus population.

$$Q^{-1} = \begin{bmatrix} \dfrac{\lambda_R}{\lambda_H} & 0 \\ 0 & \dfrac{\lambda_R}{\lambda_H} \end{bmatrix}, \quad Q_f = \begin{bmatrix} \dfrac{\lambda_R \dot{\lambda}_H - \lambda_H \dot{\lambda}_R}{\lambda_H^2} & 0 \\ 0 & \dfrac{\lambda_R \dot{\lambda}_H - \lambda_H \dot{\lambda}_R}{\lambda_H^2} \end{bmatrix}, \quad Q_f Q^{-1} = \begin{bmatrix} \dfrac{\dot{\lambda}_H}{\lambda_H} - \dfrac{\dot{\lambda}_R}{\lambda_R} & 0 \\ 0 & \dfrac{\dot{\lambda}_H}{\lambda_H} - \dfrac{\dot{\lambda}_R}{\lambda_R} \end{bmatrix}, \quad QJ^{[2]}Q^{-1} = \begin{bmatrix} \mathcal{C} & 0 \\ 0 & \mathcal{C} \end{bmatrix}.$$

We define

$$\mathcal{B} = Q_f Q^{-1} + QJ^{[2]}Q^{-1} = \begin{bmatrix} B_{11} & B_{12} \\ B_{21} & B_{22} \end{bmatrix},$$

where $B_{11} = B_{22} = \dfrac{\dot{\lambda}_H}{\lambda_H} - \dfrac{\dot{\lambda}_R}{\lambda_R} + \mathcal{C}$, $B_{12} = B_{21} = 0$.

Using

$$\frac{\dot{\lambda}_R}{\lambda_R} = \frac{\mu_2 \pi_1 b_{41} \lambda_H}{\pi_2 \lambda_R (\lambda_H + \mu_1)} + \frac{\mu_2 b_{44}}{(\lambda_R + \rho + \mu_2)} - 1,$$

Then

$$B_{11} = B_{22} = \frac{\dot{\lambda}_H}{\lambda_H} - \frac{\mu_2 \pi_1 b_{41} \lambda_H}{\pi_2 \lambda_R (\lambda_H + \mu_1)} - \frac{\mu_2 b_{44}}{(\lambda_R + \rho + \mu_2)} + 1.$$

We follow the approach in (Li & Muldowney, 1996) to get

$$\nu(\mathcal{B}) \leq sup\{g_1, g_2\} \equiv sup\{\nu_1(B_{11}) + |B_{12}|, \ \nu_1(B_{22}) + |B_{21}|\},$$

where ν_1 denotes the Lozinskii measure with respect to the L^1 norm and $|B_{12}|, |B_{21}|$ are matrix norms with respect to the L^1 vector norm. So,

$$\nu(\mathcal{B}) \leq \frac{\dot{\lambda}_H}{\lambda_H} - \frac{\mu_2 \pi_1 b_{41} \lambda_H}{\pi_2 \lambda_R (\lambda_H + \mu_1)} - \frac{\mu_2 b_{44}}{(\lambda_R + \rho + \mu_2)} + 1.$$

Using Lemma 1 in (Srivastava et al., 2022) and the uniform persistence result in (Freedman et al., 1994), this gives us
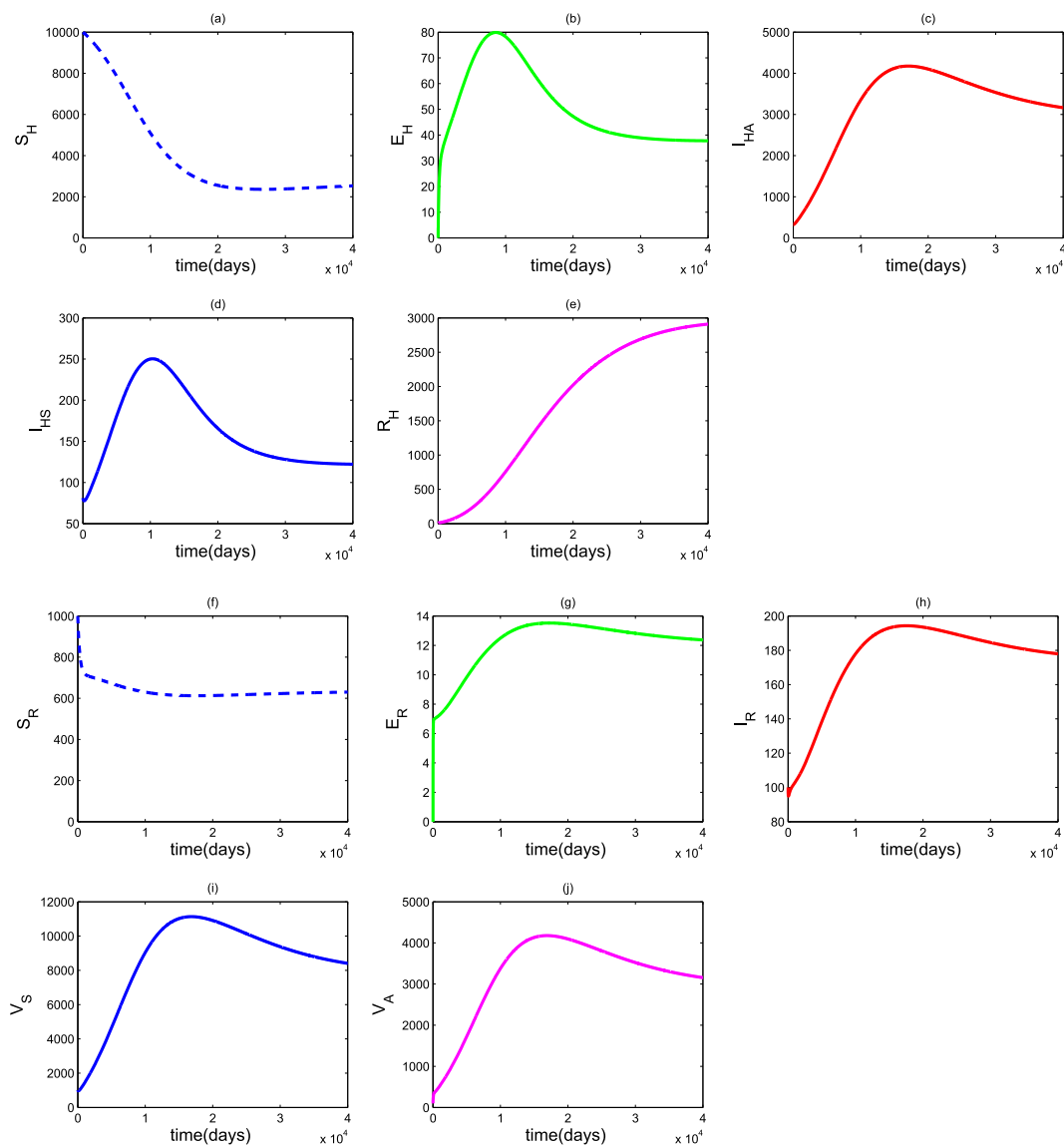
Fig. 4. Model simulations for all the state variables in model (5) with R_0 greater than unity: $R_0 = 3.1301$.

$$v(\mathscr{B}) \leq \frac{\dot{\lambda_H}}{\lambda_H} - \left\{ \frac{\mu_2 \pi_1 b_{41}}{\pi_2(c + \mu_1)} + \frac{\mu_2 b_{44}}{(c + \rho + \mu_2)} - 1 \right\}.$$

We choose $\Delta = \frac{\mu_2 \pi_1 b_{41}}{\pi_2(c+\mu_1)} + \frac{\mu_2 b_{44}}{(c+\rho+\mu_2)} - 1 > 0$, so

$$v(\mathscr{B}) \leq \frac{\dot{\lambda_H}}{\lambda_H} - \Delta.$$

Integrating both sides, we get

$$\int_0^t v(\mathscr{B}) ds \leq \int_0^t \frac{\dot{\lambda_H}}{\lambda_H} dt - \int_0^t \Delta dt,$$
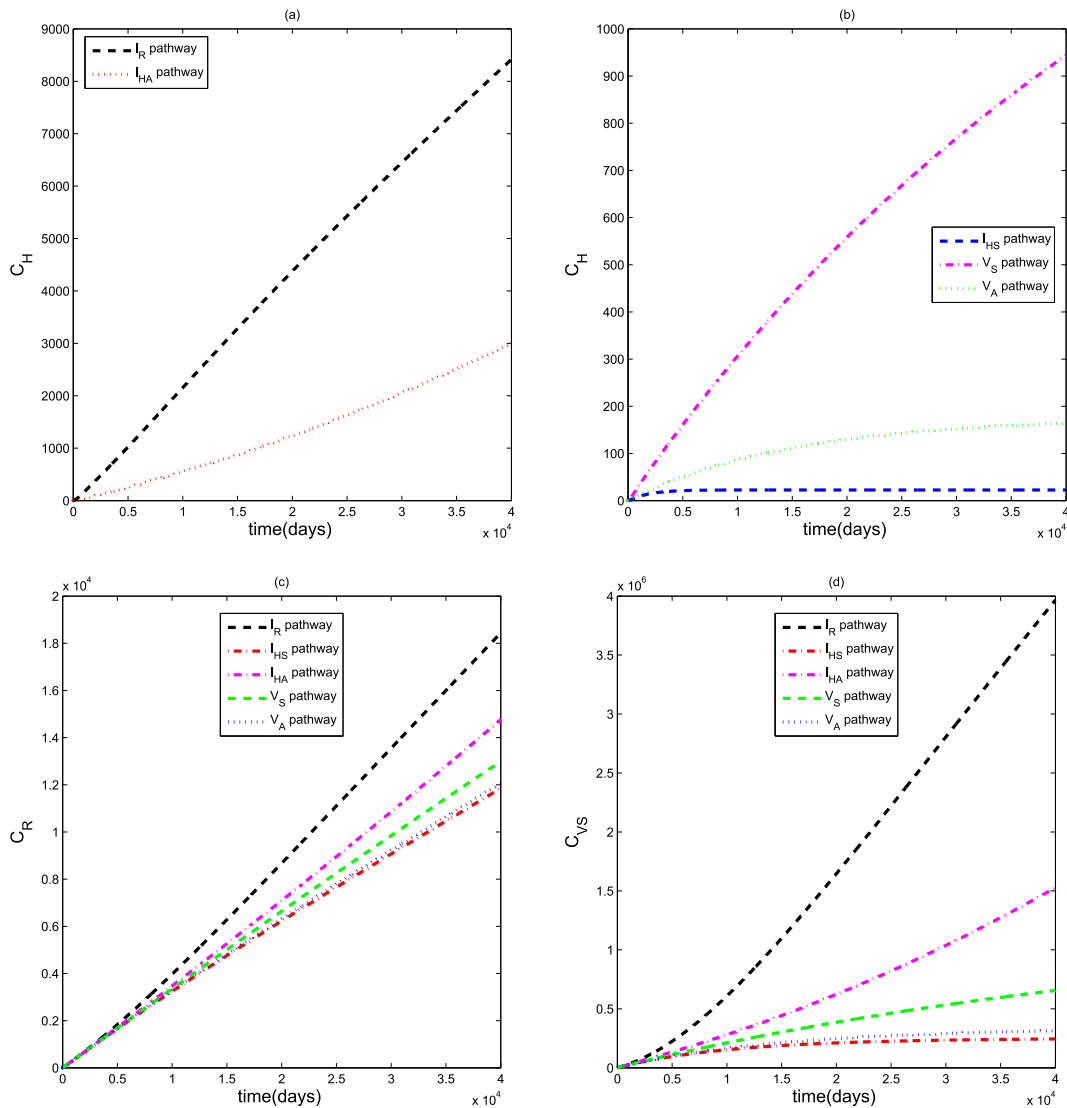
and it follows that

Fig. 5. Graphical illustration of model (5) for single transmission routes on the cumulative cases of human, rodent and virus classes.

$$\frac{1}{t}\int_0^t \nu(\mathscr{B})ds \leq \frac{1}{t}log\frac{\lambda_H(t)}{\lambda_H(0)} - \Delta,$$

or

$$\lim \sup_{t\to\infty}sup\frac{1}{t}\int_0^t \nu(\mathscr{B})ds \leq -\Delta \leq 0, \tag{17}$$

as $\lambda_H(t)$ is bounded and $\Delta > 0$

Hence, $\widehat{q_2} = \lim \sup_{t\to\infty}sup\frac{1}{t}\int_0^t \nu(\mathscr{B})ds < 0$, if $\Delta > 0$ or $\frac{\mu_2\pi_1 b_{41}}{\pi_2(c+\mu_1)} + \frac{\mu_2 b_{44}}{(c+\rho+\mu_2)} > 1$.

Thus, system (16) is globally asymptotically stable for $\frac{\mu_2\pi_1 b_{41}}{\pi_2(c+\mu_1)} + \frac{\mu_2 b_{44}}{(c+\rho+\mu_2)} > 1$, that is $(\lambda_H, \lambda_R) \to (\lambda_H^*, \lambda_R^*)$ as $t \to \infty$. $\square$

Next, we investigate conditions on the parameter values in model (5) using Center Manifold Theory (Castillo-Chavez & Song, 2004).

Theorem 2.1.4. (i) If $\frac{\beta_H\mu_2}{\pi_2}w_1\nu_2 w_1 < \frac{\beta_H\pi_1\mu_2^2}{\pi_2^2\mu_1}w_6\nu_2 w_8$ and $b > 0$, then the system (5) will undergo a forward bifurcation at $R_0 = 1$.
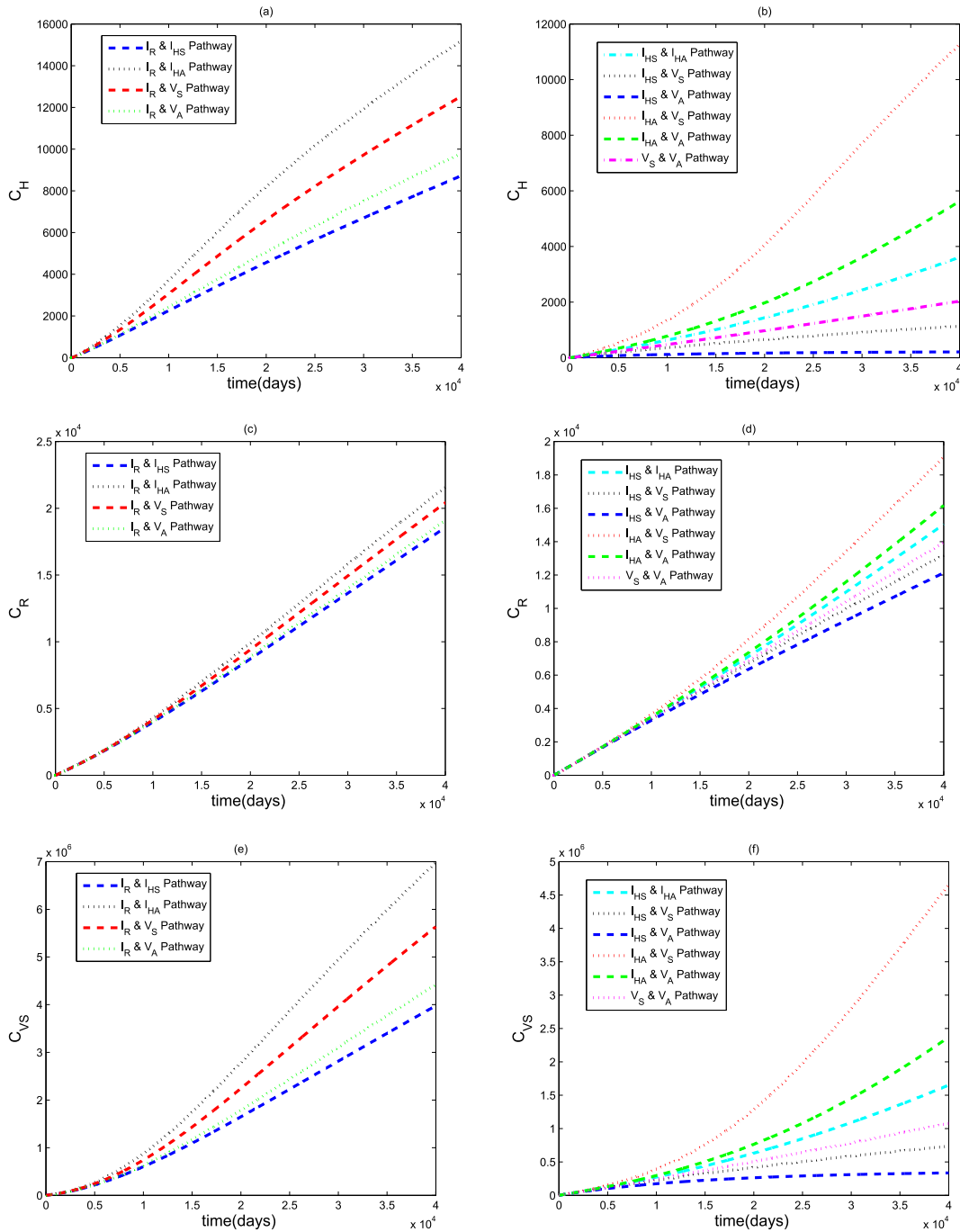
Fig. 6. Graphical illustration of model (5) for possible combination of two transmission routes on the cumulative cases of human, rodent and virus classes.

(ii) *If $B_{wv} < \frac{\beta_H \mu_2}{\pi_2} w_1 v_2 w_1 - \frac{\beta_H \pi_1 \mu_2^2}{\pi_2^2 \mu_1} w_6 v_2 w_8$, and $b > 0$, then the system (5) will undergo a backward bifurcation at $R_0 = 1$.*

(Castillo-Chavez & Song, 2004).
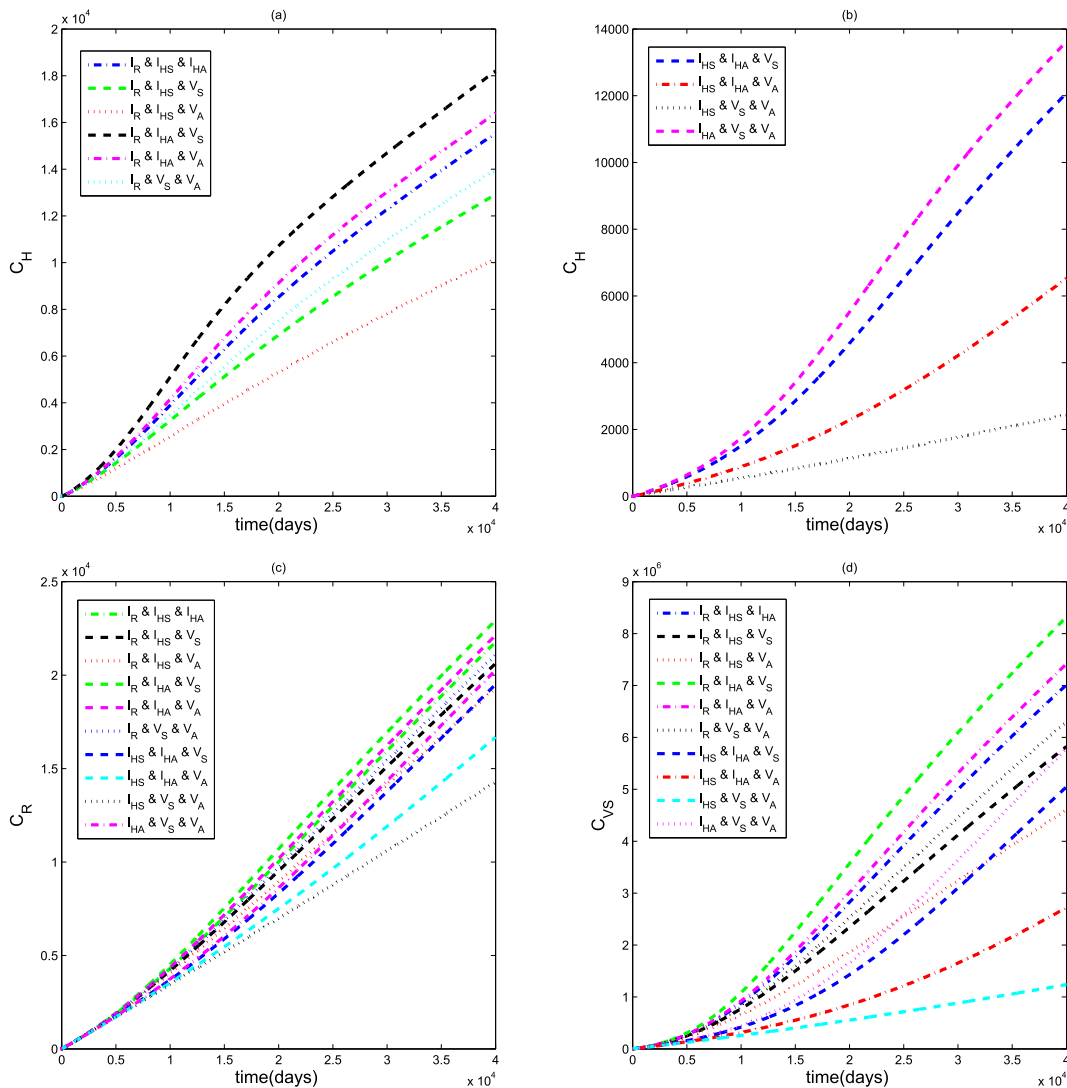
Proof. See Appendix A. □

Fig. 7. Graphical illustration of model (5) for possible combination of three transmission routes on the cumulative cases of human, rodent and virus classes.

3. Numerical simulations

3.1. Parameter estimation

It is crucial to estimate the model parameter values in order for us to perform numerical analysis. We consider the ecological niche where Lassa fever is endemic. We focus on three (3) states in Nigeria (Ondo, Edo and Ebonyi) where this virus has ravaged communities in the past few years based on Nigeria Centre for Disease Control (NCDC) reports (NCDC, 2021).

In the chosen region, we consider a few local sites in the three states of about 10000 persons, $\frac{\pi_1}{\mu_1} = 10000$. The human natural death rate is $\mu_1 = \frac{1}{55.12 \times 365}$ day^{-1} using the average human lifespan in Nigeria as 55.12 (Trends, 2021). The daily recruitment rate of humans is estimated as $\pi_1 = 10000 \times \mu_1 = 0.497$ day^{-1}. The value, $\nu = 0.8$ since 80% of individuals are asymptomatic. The sample study of Lassa fever cases in Nigeria shows a case fatality ratio of 18.9% in the year 2021 (NCDC, 2021), we assume $\delta = 0.189$ year^{-1} which translates to $\delta = 0.0005$ day^{-1}. Research conducted in these communities had reported a yearly rodent consumption rate of 29.9% in Edo State, 11% in Ebonyi State and 20.2% in Ondo State (Ossai et al., 2020; WHO, 2021). So, we use an average consumption rate of 20.4% per year giving us $\rho = 0.0006$ day^{-1}. The biological half-life of Lassa virus ranges from 10.1 to 54.6 min (Stephenson et al., 1984); so using 10.1 min implies that $\theta_3 = \frac{2 \times 10.1}{60 \times 24}$ day^{-1}.

We consider a hypothetical average population of *Mastomys* rat to be $\frac{\pi_2}{\mu_2} = 1000$, since there is no known quantified estimate of the rodents population. The average lifespan of a rodent is 1 year (Control, 2018), so we obtain $\mu_2 = \frac{1}{1 \times 365}$ day^{-1}. We estimate the rodent recruitment rate to be $\pi_2 = 1000 \times \mu_2 = 2.74$ day^{-1}. Some of the parameters cannot be found or estimated
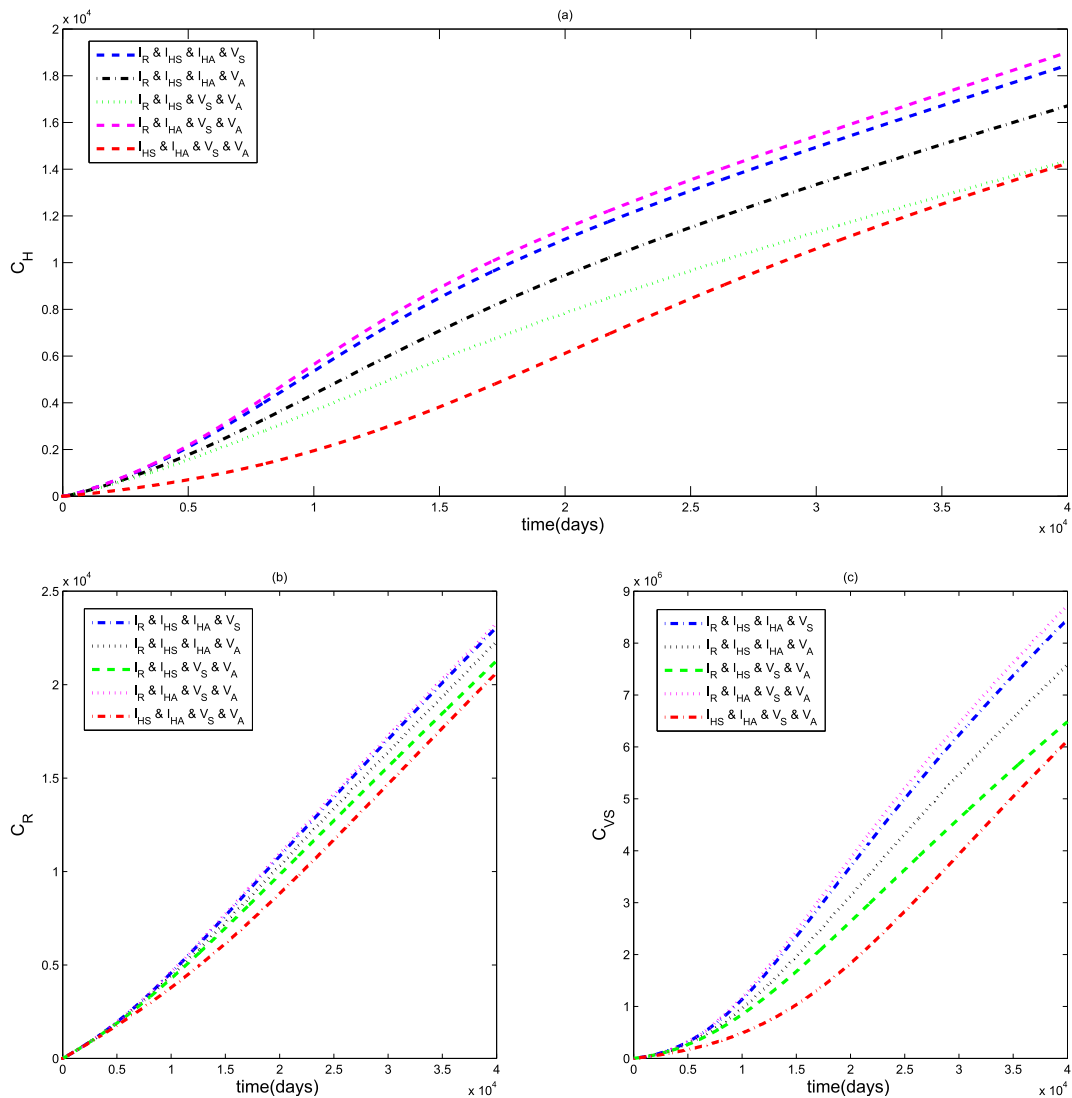
Fig. 8. Graphical illustration of model (5) for possible combination of four transmission routes on the cumulative cases of human, rodent and virus classes.

from literature, so we used model calibration to get ideal representation curves for all state variables to get approximate values. Thus $\psi_1 = 0.0094$ day^{-1}, $\psi_2 = 0.048$ day^{-1}, $\beta_H = 0.00017$ day^{-1}, $\beta_R = 0.004$ day^{-1}, $\xi = 0.167$, $\varphi_1 = \frac{1}{15}$, $\varphi_2 = \frac{1}{28}$, $\varphi_3 = \frac{3.7}{60 \times 24}$ and the values of η_1, η_2, η_3, η_4, to lie in the interval (0, 1). For our simulation, we use the following initial conditions: $S_H(0) = 10000$, $E_H(0) = 0$, $I_{HA}(0) = 324$, $I_{HS}(0) = 81$, $R_H(0) = 10$, $S_R(0) = 1000$, $E_R(0) = 0$, $I_R(0) = 100$, $V_S(0) = 1000$, $V_A(0) = 100$. Table 2 contains the parameter values used in the simulations.

3.2. Sensitivity analysis

Sensitivity analysis is a procedure used to determine the strength of model predictions to parameter values. It is crucial because there are usually flaws in assumed parameter values and generally in data collection. Sensitivity analysis shows the parameters that deserve the best numerical attention, reveals insensitive parameters that do not require much effort to estimate and shows which parameters should be targeted for intervention (Mikucki, 2012). Local sensitivity analysis is based on calculating the effect on the model output of small perturbations around a nominal parameter value. This perturbation is done on one parameter at a time using the first-order partial derivative of the model output with respect to the perturbed parameter. Here, we will investigate parameters that have a high impact on R_0, and should be targeted by intervention strategies. The global sensitivity analysis, on the other hand, seeks to explore the input parameters space across its range of variation and then quantify the input parameter importance based on a characterization of the resulting output response surface. It is a sampling-based method that investigates uncertainties for parameter values in the entire parameter range
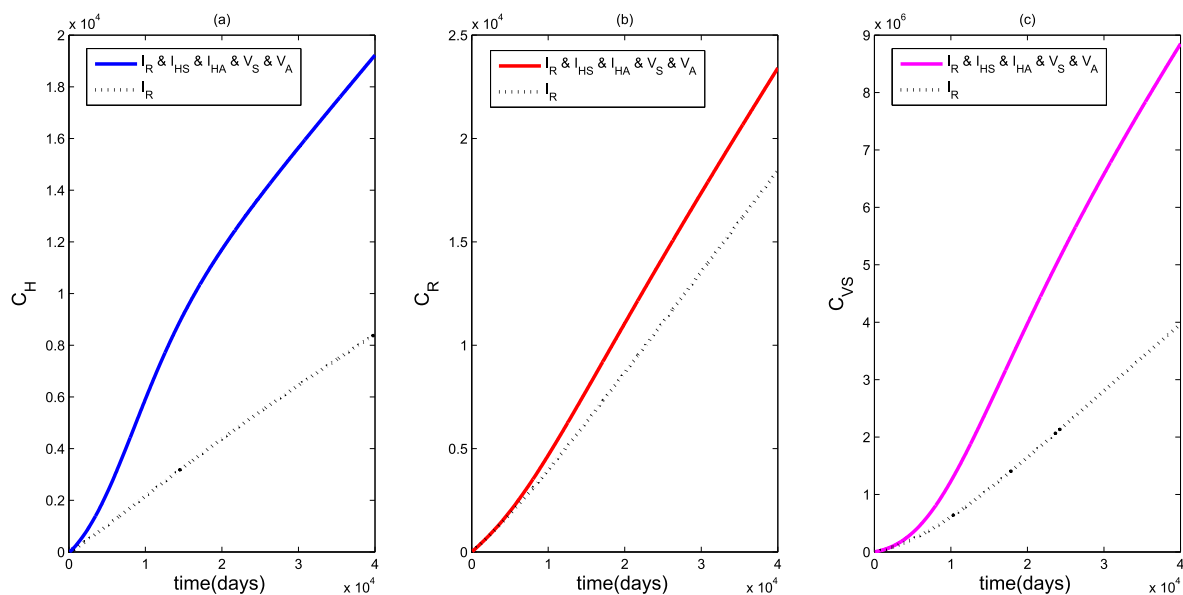
Fig. 9. Graphical illustration of model (5) for all possible combination of transmission routes alongside one transmission route on the cumulative cases of human, rodent and virus classes.

(Blower & Dowlatabadi, 1994; Marino et al., 2008; Saltelli et al., 2004, 2008; Turányi, 1990). We will perform both the local and global sensitivity analysis.

3.2.1. Local sensitivity analysis of R_0

We calculate the local sensitivity indices of the parameters with respect to R_0 using the normalized forward index. These indices reveal the importance of each parameter to disease transmission and should be taken into consideration while defining our control strategies. According to (Chitnis et al., 2008), the normalized forward sensitivity index of a variable u that depends differentiably on a parameter ρ is defined as:

$$\Upsilon_\rho^u = \frac{\partial u}{\partial \rho} \times \frac{\rho}{u}.$$

For example, the sensitivity index of R_0 with respect to β_H will be

$$\Upsilon_{\beta_H}^{R_0} = \frac{\partial R_0}{\partial \beta_H} \times \frac{\beta_H}{R_0}.$$

When $\Upsilon_{\beta_H}^{R_0} > 0$, we say that β_H increases the value of R_0 as its value increases, while if $\Upsilon_{\beta_H}^{R_0} < 0$, then β_H decreases the value of R_0 as its value increases. The results of the sensitivity indices is shown in Table 3.

We observe from Table 3 that parameters such as β_H, ν, η_2, π_1, φ_1, η_3, η_4, η_1, β_R, ξ_1 are positively correlated with R_0 thus increase in these parameters increase the reproduction number. The parameters μ_1, ζ_1, δ, θ_2 are negatively correlated with R_0 thus they decrease the value of R_0 as they are increased. There are parameters such as π_2, μ_2, ρ, φ_3 that are insensitive with respect to the reproduction number of Lassa fever in the population. These parameters do not require too much effort to estimate and will not cause much changes to R_0 when they are increased or decreased. All parameters associated with infection pathways have positive indices and thus, all the infection pathways have a potential to collectively or otherwise increase the infection. We also observe that β_H is the most sensitive parameter followed by ν, η_2, π_1, φ_1, η_3, η_4, η_1, β_R, ξ_1 respectively. Intervention strategies can be targeted at reducing the impact of parameters which increase R_0 whilst increasing those that reduce it.

3.2.2. Global sensitivity analysis

The global sensitivity analysis is carried out using the Latin Hypercube Sampling and Partial Rank Correlation Coefficients (PRCCs) (Marino et al., 2008). This is a robust sensitivity measure that combines uncertainty analysis with partial correlation on rank-transformed data to assess the sensitivity of our outcome variable to parameter variation. Figs. 2 and 3 shows that the parameters β_H, β_R, φ_1, φ_3, θ_3, ψ_1, ν are positively correlated to C_H and thus increase the burden of Lassa fever infection in the human population; the parameters θ_2, μ_2, π_1 are negatively correlated to C_H and decrease the burden of Lassa virus in the
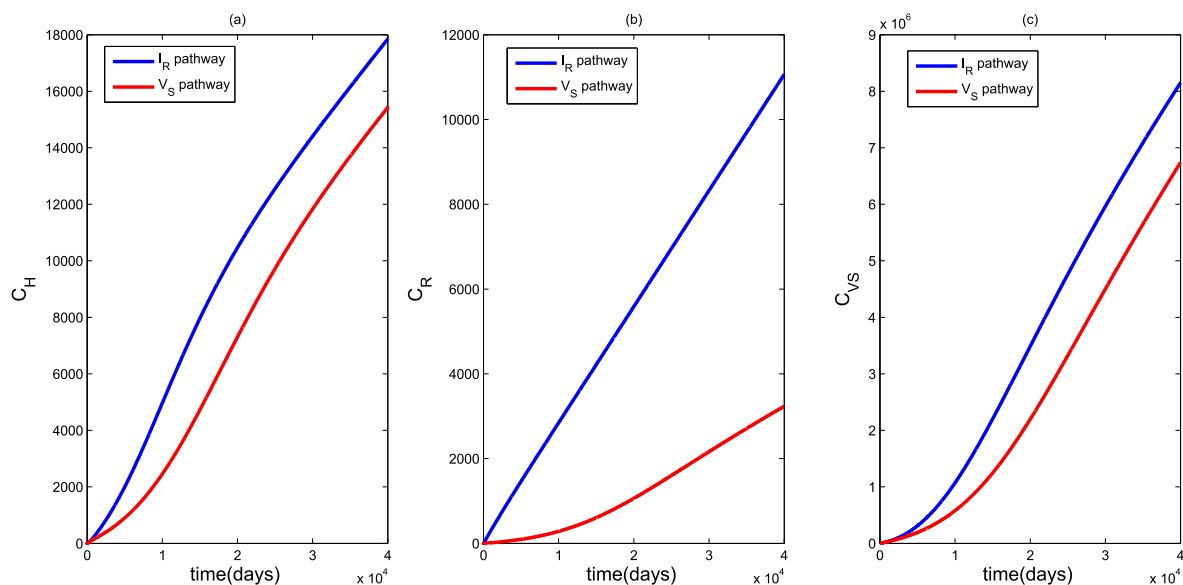
Fig. 10. Graphical illustration of model (5) for possible combination of the two rodent transmission routes on all the classes.

human population when they are increased. There are also insensitive parameters ψ_2, μ_1, ψ_1, ζ_1, ζ_2, φ_2 with PRCCs very close to zero. The parameters associated with infection pathways though weakly correlated, remain positively correlated in the different populations. In the rodent population, the parameters β_H, β_R, ψ_1, ψ_2, μ_1, μ_2, θ_3 are positively correlated to C_R and increase the infection burden in rodents, parameters π_1, π_2, μ_2, φ_2, ρ, μ_2, θ_3 are negatively correlated to C_R while there are parameters with PRCCs close to zero such as δ, θ_3, ζ_1, ζ_2 and so on. From the PRCCs of the virus population, we see positively correlated parameters such as β_R, ψ_2, π_2, μ_1, ξ_1, negatively correlated parameters μ_2, ρ, π_1 and other parameters with PRCCs very close to zero. In all populations, we see that some parameters are positively or negatively correlated at certain time points but become insensitive at other time points and verse visa. Hence, the interplay and the exchange of sensitivity by different parameters on different variables alludes to the complexities brought about by the multiple transmission pathways which in turn suggest the importance of every pathway in the prognosis of Lassa fever.

3.3. Simulation results

Fig. 4 shows the baseline graphs of system (5) without varying the system parameters. The simulations were done over a time period of 40000 days. The baseline graph is perceived to represent the ideal situation where Lassa fever persists in the system. We will illustrate the impact of the transmission pathways in the next subsection.

3.3.1. Simulation of the transmission pathways

We now investigate the impact of the various transmission routes on the progression of Lassa fever in both human and rodent population as well as the growth of virus in the environment. We shall proceed using the following strategies:

1. Transmission pathways for the human population
   (a) 5 Single transmission pathways (see Fig. 5).
   (b) 10 combinations of two transmission pathways (see Fig. 6).
   (c) 10 combinations of three transmission pathways (see Fig. 7).
   (d) 5 combinations of four transmission pathways (see Fig. 8).
   (e) 1 combination of five transmission pathways (see Fig. 9).
2. Transmission pathways for rodent population
   (a) Single transmission pathways (see Fig. 9).
   (b) 1 combination of two transmission pathways (see Fig. 10).

By single transmission pathway, we use each of the single contact rates in the human force of infection and test its impact on the system while the entire rodent force of infection is operational. We do the same for two transmission routes and continue till we exhaust all other transmission pathways. We also investigate using each of the single contact rates in the rodent force of infection and the two transmission routes while keeping the entire human force of infection in use. We shall

test these strategies using the cumulative cases (NCDC, 2021) in the humans, rodents and virus in the environment. To capture this, we will simulate the cumulative cases using the equations:

$$
\begin{aligned}
\frac{dC_H}{dt} &= \psi_1 E_H, \\
\frac{dC_R}{dt} &= \psi_2 E_R, \\
\frac{dC_{V_S}}{dt} &= \varphi_1 I_{HA} + \varphi_2 I_{HS} + \varphi_3 I_R,
\end{aligned}
\tag{19}
$$

subject to the initial conditions $C_H(0) = 0$, $C_R(0) = 0$, $C_{V_s}(0) = 505$, where C_H is the cumulative infection cases in the human population, C_R is the cumulative infection cases in the rodent population, and C_{VS} is the cumulative infection cases in the virus population.

Fig. 5 reveals that the effective contact rate between susceptible humans and infected rodents does the most damage with regards to the progression of infection. This is followed by the contact rate between susceptible humans and infectious asymptomatic humans which is less infectious and then by the contact with contaminated environment, contaminated air, and infectious symptomatic humans. We observe that every single route of transmission plays a role in driving the Lassa fever infection even though some are less significant than the others. In the rodent population, we also see a notable difference in the level of infectiousness of the transmission routes likewise in the virus population. This shows that some pathways are more deadly than others yet every pathway makes their own contribution. We see from Fig. 6 that a combination of two transmission pathways increases disease burden more than a single pathway. We also see that some combinations are more deadly than others. Any combination with the effective contact rate between susceptible humans and infected rodents produces a surge of infections followed by any combination with the effective contact rate between susceptible humans and infectious asymptomatic humans and then other pathways. Overall, we see that as the number of transmission routes increase, the burden of infection increases also (see Figs. 7—8). Fig. 9 shows a combination of all the transmission routes plotted alongside the dominant single transmission pathway. The region between the two graphs accounts for the contribution of other pathways in combination with the effective contact rate between susceptible humans and infected rodents. This shows that even though the effective contact rate between susceptible humans and infected rodents is dominant, other pathways should not be neglected because when they work in combination, there is an additional increase in the burden of Lassa fever over a cumulative period of time. It is also important to note that horizontal transmissions between susceptible rodents and infected rodents also play a huge role in increasing the infection as well as contact rate between susceptible rodent and contaminated environmental surfaces (see Fig. 10).

3.4. Discussion of results

We investigated the transmission dynamics of Lassa fever infection incorporating multiple transmission routes to capture their impact on the progression of the infection. Using a deterministic model that accounts for Lassa fever infection, we were able to show how incorporating several transmission pathways affects the prevalence of the disease. We used some mathematical tools to establish the local stability of the endemic equilibrium and the global stability of the disease free equilibrium. From our analysis, we got mathematical expressions that shows the conditions for which the disease will persist or be controlled in the system and illustrated sensitivity of parameters changes as system dynamics progress.

From our model simulations, we see that every transmission pathway has an impact towards the progression of Lassa fever. However, there are some routes of transmission that contribute significantly more than others. Control measures should be targeted more on the contact rates between susceptible humans and infected rodents (especially in areas where rodent consumption is high), and contact rates between susceptible humans and infectious asymptomatic humans. A great challenge arises when dealing with susceptible and asymptomatic infected humans pathway because they are not easily identified through symptoms. This calls for control methods that can detect this category of people such as mass testings in endemic areas, vaccination and so on. It is also important not to neglect the contact rates between susceptible humans and contaminated air particles especially in health centres with recorded Lassa fever cases and the contact rates between susceptible humans and contaminated environment (especially in poorly sanitized areas) because they are further drivers of infection (CDC, 2014).

Most single transmission routes are less harmful, but when they operate in combination with other transmission routes, they contribute additional damage to the system. Studies (Ibrahim & Dénes, 2021; Ojo et al., 2021; Onah et al., 2020; Peter et al., 2020) that only concentrated on the human and rodent direct transmission routes have not captured valuable information on the environmental impact towards the progression of the infection. This work gives a more comprehensive breakdown of the transmission dynamics of Lassa fever as it integrates indirect transmission routes which are sometimes neglected but play a crucial role in increasing the infection statistics. Current reports show that about four medical doctors died and 38 health workers were infected during a recent Lassa fever outbreak in Nigeria (NCDC, 2022; Punch, 2022). This increase in the death of health workers tells of the fact that serious measures should be taken to curb the spread of the virus through the indirect transmission routes like the environmental surfaces and aerosol. This will help to reduce the impact of

these indirect transmission routes on the infection chain. Public health agencies in Nigeria have done a lot in mitigating Lassa fever infection through administering Ribavirin, public awareness campaigns amongst others. A lot still needs to be done in endemic areas by adequate fumigation of the environment and provision of protective gears for health workers. The results from our work show that interventions on these areas should not be undermined during health policy making. Further studies can be targeted at.

- combination of multiple routes of transmission incorporating the effect of seasonality of infection,
- proper sanitation, intervention strategies and holistic control measures that integrate these multiple transmission pathways which can help public health reduce disease prevalence,
- optimizing cost of several control measures using Cost Effective Analysis so that individuals in endemic areas with issues of poverty can be properly assisted.

Access to real field data can also improve the predictive capacity of the current model. Vertical transmission of Lassa fever in rodents can also be incorporated in further studies. Alternative techniques like the scaling of the model can be used to help simplify the analysis where parameters are dimensionless and express ratios of physical effects rather than levels of individual effects(Ledder, 2017).

Declaration of competing interest

The Authors declare no conflict of interest in this work.

Appendix A. Sample Appendix Section

Proof. Let $x_i = (x_1, x_2, x_3, x_4, x_5, x_6, x_7, x_8, x_9, x_{10})^T = (S_H, E_H, I_{HA}, I_{HS}, R_H, S_R, E_R, I_R, V_S, V_A)^T$.
Then, model (5) can be written in the form $\frac{dx_i}{dt} = g(x)$ as follows:

$$
\begin{aligned}
\frac{dx_1}{dt} &= g_1 = \pi_1 - \lambda_H x_1 - \mu_1 x_1, \\
\frac{dx_2}{dt} &= g_2 = \lambda_H x_1 - (\psi_1 + \mu_1) x_2, \\
\frac{dx_3}{dt} &= g_3 = \nu \psi_1 x_2 - (\zeta_1 + \mu_1) x_3, \\
\frac{dx_4}{dt} &= g_4 = (1 - \nu)\psi_1 x_2 - (\delta + \zeta_2 + \mu_1) x_4, \\
\frac{dx_5}{dt} &= g_5 = \zeta_1 x_3 + \zeta_2 x_4 - \mu_1 x_5, \\
\frac{dx_6}{dt} &= g_6 = \pi_2 - \lambda_R x_6 - (\rho + \mu_2) x_6, \\
\frac{dx_7}{dt} &= g_7 = \lambda_R x_6 - (\psi_2 + \rho + \mu_2) x_7, \\
\frac{dx_8}{dt} &= g_8 = \psi_2 x_7 - (\rho + \mu_2) x_8, \\
\frac{dx_9}{dt} &= g_9 = \varphi_1 x_3 + \varphi_2 x_4 + \varphi_3 x_8 - (\theta_2 + \theta_3) x_9, \\
\frac{dx_{10}}{dt} &= g_{10} = \theta_3 x_9 - \theta_2 x_{10},
\end{aligned}
\tag{A.1}
$$

where

$$
\begin{aligned}
\lambda_H &= \frac{\beta_H x_8}{x_6 + x_7 + x_8} + \frac{\beta_H \eta_1 x_4}{x_1 + x_2 + x_3 + x_4 + x_5} + \frac{\beta_H \eta_2 x_3}{x_1 + x_2 + x_3 + x_4 + x_5} + \frac{\beta_H \eta_3 x_9}{K_V} \\
&\quad + \frac{\beta_H \eta_4 x_{10}}{K_V}, \\
\lambda_R &= \beta_R \left(\frac{x_8}{x_6 + x_7 + x_8} + \frac{\xi_1 x_9}{K_V} \right).
\end{aligned}
$$

We choose β_H as the bifurcation parameter by setting $R_0 = 1$. To do this, we let $\beta_R \propto \beta_H$ which implies that $\beta_R = \tau \beta_H$ for some $\tau > 0$. Then from the value of R_0 we get

$$\beta_H = \beta_H^* = \frac{2}{\beta_{H1}^* + \beta_{H4}^* + \sqrt{(\beta_{H1}^* - \beta_{H4}^*)^2 + 4\beta_{H2}^*\beta_{H3}^*}}, \tag{A.2}$$

where

$$
\begin{aligned}
\beta_{H1}^* &= \frac{K_V\theta_2(\theta_2+\theta_3)\mu_1(\eta_2(\delta+\zeta_2+\mu_1)\nu\psi_1 - (-1+\nu)\eta_1(\zeta_1+\mu_1)\psi_1)}{K_V\theta_2(\theta_2+\theta_3)\mu_1(\zeta_1+\mu_1)(\delta+\zeta_2+\mu_1)(\mu_1+\psi_1)} \\
&\quad + \frac{\pi_1(\eta_3\theta_2+\eta_4\theta_3)((\delta+\zeta_2+\mu_1)\nu\psi_1\varphi_1 - (-1+\nu)(\zeta_1+\mu_1)\varphi_2\psi_1))}{K_V\theta_2(\theta_2+\theta_3)\mu_1(\zeta_1+\mu_1)(\delta+\zeta_2+\mu_1)(\mu_1+\psi_1)}, \\
\beta_{H2}^* &= \frac{\pi_1(K_V\theta_2(\theta_2+\theta_3)\mu_2 + \pi_2(\eta_3\theta_2+\eta_4\theta_3)\varphi_3)\psi_2}{K_V\pi_2\theta_2(\theta_2+\theta_3)\mu_1(\rho+\psi_2)(\mu_2+\rho+\psi_2)}, \\
\beta_{H3}^* &= \frac{\pi_2\tau\xi_1((\delta+\zeta_2+\mu_1)\nu\psi_1\varphi_1 - (-1+\nu)(\zeta_1+\mu_1)\varphi_2\psi_1)}{K_V(\theta_2+\theta_3)(\zeta_1+\mu_1)(\delta+\zeta_2+\mu_1)\mu_2(\mu_1+\psi_1)}, \\
\beta_{H4}^* &= \frac{\tau(K_V(\theta_2+\theta_3)\mu_2 + \pi_2\xi_1\varphi_3)\psi_2}{K_V(\theta_2+\theta_3)\mu_2(\rho+\psi_2)(\mu_2+\rho+\psi_2)}.
\end{aligned}
$$

The Jacobian of system (8) evaluated at the DFE E_0 with the bifurcation parameter β_H^* donated by J_{E_0} is given as

$$
\begin{pmatrix}
-\mu_1 & 0 & -\beta_H^*\eta_2 & -\beta_H^*\eta_1 & 0 & 0 & 0 & -\dfrac{\beta_H^*\mu_2\pi_1}{\mu_1\pi_2} & -\dfrac{\beta_H^*\eta_3\pi_1}{\mu_1 K_V} & -\dfrac{\beta_H^*\eta_4\pi_1}{\mu_1 K_V} \\
0 & j_{22} & \beta_H^*\eta_2 & \beta_H^*\eta_1 & 0 & 0 & 0 & \dfrac{\beta_H^*\mu_2\pi_1}{\mu_1\pi_2} & \dfrac{\beta_H^*\eta_3\pi_1}{\mu_1 K_V} & \dfrac{\beta_H^*\eta_4\pi_1}{\mu_1 K_V} \\
0 & \nu\psi_1 & j_{33} & 0 & 0 & 0 & 0 & 0 & 0 & 0 \\
0 & (1-\nu)\psi_1 & 0 & j_{44} & 0 & 0 & 0 & 0 & 0 & 0 \\
0 & 0 & \zeta_1 & \zeta_2 & -\mu_1 & 0 & 0 & 0 & 0 & 0 \\
0 & 0 & 0 & 0 & 0 & -(\rho+\mu_2) & 0 & -\tau\beta_H^* & -\dfrac{\tau\beta_H^*\xi_1\pi_2}{\mu_2 K_V} & 0 \\
0 & 0 & 0 & 0 & 0 & 0 & j_{77} & \tau\beta_H^* & \dfrac{\tau\beta_H^*\xi_1\pi_2}{\mu_2 K_V} & 0 \\
0 & 0 & 0 & 0 & 0 & 0 & \psi_2 & j_{88} & 0 & 0 \\
0 & 0 & \varphi_1 & \varphi_2 & 0 & 0 & 0 & \varphi_3 & -(\theta_2+\theta_3) & 0 \\
0 & 0 & 0 & 0 & 0 & 0 & 0 & 0 & \theta_3 & -\theta_2
\end{pmatrix}.
$$

where

$$j_{22} = -(\psi_1+\mu_1), \quad j_{33} = -(\zeta_1+\mu_1), \quad j_{44} = -(\delta+\zeta_2+\mu_1), \quad j_{77} = -(\psi_2+\rho+\mu_2), \quad j_{88} = -(\rho+\mu_2).$$

A right eigenvector associated with the zero eigenvalue is given by

$$w = (w_1, w_2, w_3, w_4, w_5, w_6, w_7, w_8, w_9, w_{10})^T.$$

We get it from the following equations:

$$-\mu_1 w_1 - \beta_H^* \eta_2 w_3 - \beta_H^* \eta_1 w_4 - \frac{\mu_2 \pi_1}{\mu_1 \pi_2}\beta_H^* w_8 - \frac{\beta_H^* \eta_3 \pi_1}{\mu_1 K_V}w_9 - \frac{\beta_H^* \eta_4 \pi_1}{\mu_1 K_V}w_{10} = 0$$

$$-(\psi_1 + \mu_1)w_2 + \beta_H \eta_2 w_3 + \beta_H^* \eta_1 w_4 + \frac{\mu_2 \pi_1}{\mu_1 \pi_2}\beta_H^* w_8 + \frac{\beta_H^* \eta_3 \pi_1}{\mu_1 K_V}w_9 + \frac{\beta_H^* \eta_4 \pi_1}{\mu_1 K_V}w_{10} = 0 \nu\psi_1 w_2 - (\zeta_1 + \mu_1)w_3 = 0$$

$$(1 - \nu)\psi_1 w_2 - (\delta + \zeta_2 + \mu_1)w_4 = 0$$

$$\zeta_1 w_3 + \zeta_2 w_4 - \mu_1 w_5 = 0 - (\rho + \mu_2)w_6 - \tau\beta_H^* w_8 - \frac{\tau\beta_H^* \xi_1 \pi_2}{\mu_2 K_V}w_9 = 0 - (\psi_2 + \rho + \mu_2)w_7 + \tau\beta_H^* w_8 + \frac{\tau\beta_H^* \xi_1 \pi_2}{\mu_2 K_V}w_9 = 0$$

$$\psi_2 w_7 - (\rho + \mu_2)w_8 = 0$$

$$\varphi_1 w_3 + \varphi_2 w_4 + \varphi_3 w_8 - (\theta_2 + \theta_3)w_9 = 0$$

$$\theta_3 w_9 - \theta_2 w_{10} = 0$$

$$\text{(A.3)}$$

The solution to (A.3) gives

$$
\begin{aligned}
w_1 &= -\frac{\beta_H^* \eta_2 w_3}{\mu_1} - \frac{\beta_H^* \eta_1 w_4}{\mu_1} - \frac{\beta_H^* \mu_2 \pi_1}{\mu_1^2 \pi_2}w_8 - \frac{\beta_H^* \eta_3 \pi_1}{\mu_1^2 K_V}w_9 - \frac{\beta_H^* \eta_4 \pi_1}{\mu_1^2 K_V}w_{10}, \\
w_2 &= w_2 > 0, \ w_3 = \frac{\nu\psi_1 w_2}{\zeta_1 + \mu_1}, \ w_4 = \frac{(1-\nu)\psi_1 w_2}{\delta + \zeta_2 + \mu_1}, \ w_5 = \frac{\zeta_1 w_3 + \zeta_2 w_4}{\mu_1}, \\
w_6 &= -\frac{\tau\beta_H^* w_8}{\rho + \mu_2} - \frac{\tau\beta_H^* \xi_1 \pi_2}{\mu_2 K_V(\rho + \mu_2)}w_9, \ w_7 = \frac{\tau\beta_H^* w_8}{\psi_2 + \rho + \mu_2} + \frac{\tau\beta_H^* \xi_1 \pi_2}{\mu_2 K_V(\psi_2 + \rho + \mu_2)}w_9, \\
w_8 &= \frac{\psi_2 w_7}{\rho + \mu_2}, \ w_9 = \frac{\varphi_1 w_3 + \varphi_2 w_4 + \varphi_3 w_8}{(\theta_2 + \theta_3)}, \ w_{10} = \frac{\theta_3 w_9}{\theta_2}.
\end{aligned}
$$

$$\text{(A.4)}$$

Similarly, a left eigenvector (associated with the zero eigenvalue) given by

$$v = (v_1, v_2, v_3, v_4, v_5, v_6, v_7, v_8, v_9, v_{10})^T,$$

which satisfies $v.w = 1$ is obtained by the transpose of the matrix J_{E_0} which is

$$
\begin{pmatrix}
-\mu_1 & 0 & 0 & 0 & 0 & 0 & 0 & 0 & 0 & 0 \\
0 & j_{22}^T & \nu\psi_1 & (1-\nu)\psi_1 & 0 & 0 & 0 & 0 & 0 & 0 \\
-\beta_H^* \eta_2 & \beta_H^* \eta_2 & j_{33}^T & 0 & \zeta_1 & 0 & 0 & 0 & \varphi_1 & 0 \\
-\beta_H^* \eta_1 & \beta_H^* \eta_1 & 0 & j_{44}^T & \zeta_2 & 0 & 0 & 0 & \varphi_2 & 0 \\
0 & 0 & 0 & 0 & -\mu_1 & 0 & 0 & 0 & 0 & 0 \\
0 & 0 & 0 & 0 & 0 & -(\rho + \mu_2) & 0 & 0 & 0 & 0 \\
0 & 0 & 0 & 0 & 0 & 0 & j_{77}^T & \psi_2 & 0 & 0 \\
-\dfrac{\beta_H^* \mu_2 \pi_1}{\mu_1 \pi_2} & \dfrac{\beta_H^* \mu_2 \pi_1}{\mu_1 \pi_2} & 0 & 0 & 0 & -\tau\beta_H^* & \tau\beta_H^* & j_{88}^T & \varphi_3 & 0 \\
-\dfrac{\beta_H^* \eta_3 \pi_1}{\mu_1 K_V} & \dfrac{\beta_H^* \eta_3 \pi_1}{\mu_1 K_V} & 0 & 0 & 0 & -\dfrac{\tau\beta_H^* \xi_1 \pi_2}{\mu_2 K_V} & \dfrac{\tau\beta_H^* \xi_1 \pi_2}{\mu_2 K_V} & 0 & -(\theta_2 + \theta_3) & \theta_3 \\
-\dfrac{\beta_H^* \eta_4 \pi_1}{\mu_1 K_V} & \dfrac{\beta_H^* \eta_4 \pi_1}{\mu_1 K_V} & 0 & 0 & 0 & 0 & 0 & 0 & 0 & -\theta_2
\end{pmatrix}.
$$

where

$$j_{22}^T = -(\psi_1 + \mu_1), \quad j_{33}^T = -(\zeta_1 + \mu_1), \quad j_{44}^T = -(\delta + \zeta_2 + \mu_1), \quad j_{77}^T = -(\psi_2 + \rho + \mu_2), \quad j_{88}^T = -(\rho + \mu_2).$$

The system of equations obtained is given by

$$-\mu_1 v_1 = 0 - (\psi_1 + \mu_1)v_2 + \nu\psi_1 v_3 + (1-\nu)\psi_1 v_4$$

$$= 0 - \beta_H^* \eta_2 v_1 + \beta_H^* \eta_2 v_2 - (\zeta_1 + \mu_1)v_3 + \zeta_1 v_5 + \varphi_1 v_9$$

$$= 0 - \beta_H^* \eta_1 v_1 + \beta_H^* \eta_1 v_2 - (\delta + \zeta_2 + \mu_1)v_4 + \zeta_2 v_5 + \varphi_2 v_9$$

$$= 0 - \mu_1 v_5$$

$$= 0 - (\rho + \mu_2)v_6$$

$$= 0 - (\psi_2 + \rho + \mu_2)v_7 + \psi_2 v_8 \qquad\qquad (A.4)$$

$$= 0 - \frac{\beta_H^* \mu_2 \pi_1}{\mu_1 \pi_2}v_1 + \frac{\beta_H^* \mu_2 \pi_1}{\mu_1 \pi_2}v_2 - \tau\beta_H^* v_6 + \tau\beta_H^* v_7 - (\rho + \mu_2)v_8 + \varphi_3 v_9$$

$$= 0 - \frac{\beta_H^* \eta_3 \pi_1}{\mu_1 K_V}v_1 + \frac{\beta_H^* \eta_3 \pi_1}{\mu_1 K_V}v_2 - \frac{\tau\beta_H^* \xi_1 \pi_2}{\mu_2 K_V}v_6 + \frac{\tau\beta_H^* \xi_1 \pi_2}{\mu_2 K_V}v_7 - (\theta_2 + \theta_3)v_9 + \theta_3 v_{10}$$

$$= 0 - \frac{\beta_H^* \eta_4 \pi_1}{\mu_1 K_V}v_1 + \frac{\beta_H^* \eta_4 \pi_1}{\mu_1 K_V}v_2 - \theta_2 v_{10}$$

$$= 0$$

Solving (A.4) gives

$$v_1 = 0,\ v_2 = v_2 > 0,\ v_3 = \frac{\beta_H^* \eta_2 v_2 + \varphi_1 v_9}{\zeta_1 + \mu_1},\ v_4 = \frac{\beta_H^* \eta_1 v_2 + \varphi_2 v_9}{\delta + \zeta_2 + \mu_1},\ v_5 = 0,\ v_6 = 0,\ v_7 = \frac{\psi_2 v_8}{\psi_2 + \rho + \mu_2},$$

$$v_8 = \frac{\tau\beta_H^* v_7}{\rho + \mu_2} + \frac{\beta_H^* \mu_2 \pi_1 v_2}{\mu_1 \pi_2 (\rho + \mu_2)} + \frac{\varphi_3 v_9}{\rho + \mu_2},\ v_9 = \frac{\beta_H^* \eta_3 \pi_1 v_2}{\mu_1 K_V(\theta_2 + \theta_3)} + \frac{\tau\beta_H^* \xi_1 \pi_2 v_7}{\mu_2 K_V(\theta_2 + \theta_3)} + \frac{\theta_3 v_{10}}{\theta_2 + \theta_3},\ v_{10} = \frac{\beta_H^* \eta_4 \pi_1 v_2}{\theta_2 \mu_1 K_V}.$$

We use the property $v.w = 1$ to get

$$v_1 w_1 + v_2 w_2 + v_3 w_3 + v_4 w_4 + v_5 w_5 + v_6 w_6 + v_7 w_7 + v_8 w_8 + v_9 w_9 + v_{10} w_{10} = 1.$$

Choosing $w_2 = 1$ without loss of generality gives us

$$v_2 = \frac{1}{1 + (A_3 w_3 + A_4 w_4 + A_7 w_7 + A_8 w_8 + A_9 w_9 + A_{10} w_{10})} > 0,$$

where

$$A_3 = \frac{\beta_H\left(\eta_2 + \dfrac{\pi_1\mu_2\varphi_1\left(\tau\beta_H\theta_2\xi_1\psi_2 + \eta_3\theta_2\left(\rho^2 + \mu_2^2 + (\rho - \tau\beta_H)\psi_2 + \mu_2(2\rho + \psi_2)\right) + \eta_4\theta_3\left(\rho^2 + \mu_2^2 + (\rho - \tau\beta_H)\psi_2 + \mu_2(2\rho + \psi_2)\right)\right)}{\theta_2\mu_1\left(-\tau\pi_2\beta_H\xi_1\varphi_3\psi_2 + K_V(\theta_2 + \theta_3)\mu_2\left(\rho^2 + \mu_2^2 + (\rho - \tau\beta_H)\psi_2 + \mu_2(2\rho + \psi_2)\right)\right)}\right)}{\zeta_1 + \mu_1},$$

$$A_4 = \frac{\beta_H\left(\eta_1 + \dfrac{\pi_1\mu_2\varphi_2\left(\tau\beta_H\theta_2\xi_1\psi_2 + \eta_3\theta_2\left(\rho^2 + \mu_2^2 + (\rho - \tau\beta_H)\psi_2 + \mu_2(2\rho + \psi_2)\right) + \eta_4\theta_3\left(\rho^2 + \mu_2^2 + (\rho - \tau\beta_H)\psi_2 + \mu_2(2\rho + \psi_2)\right)\right)}{\theta_2\mu_1\left(-\tau\pi_2\beta_H\xi_1\varphi_3\psi_2 + K_V(\theta_2 + \theta_3)\mu_2\left(\rho^2 + \mu_2^2 + (\rho - \tau\beta_H)\psi_2 + \mu_2(2\rho + \psi_2)\right)\right)}\right)}{\delta + \zeta_2 + \mu_1},$$

$$A_7 = -\frac{\pi_1\beta_H\mu_2(K_V\theta_2(\theta_2 + \theta_3)\mu_2 + \pi_2(\eta_3\theta_2 + \eta_4\theta_3)\varphi_3)\psi_2}{\pi_2\theta_2\mu_1\left(\tau\pi_2\beta_H\xi_1\varphi_3\psi_2 - K_V(\theta_2 + \theta_3)\mu_2\left(\rho^2 + \mu_2^2 + (\rho - \tau\beta_H)\psi_2 + \mu_2(2\rho + \psi_2)\right)\right)},$$

$$A_8 = -\frac{\pi_1\beta_H\mu_2(K_V\theta_2(\theta_2 + \theta_3)\mu_2 + \pi_2(\eta_3\theta_2 + \eta_4\theta_3)\varphi_3)(\rho + \mu_2 + \psi_2)}{\pi_2\theta_2\mu_1\left(\tau\pi_2\beta_H\xi_1\varphi_3\psi_2 - K_V(\theta_2 + \theta_3)\mu_2\left(\rho^2 + \mu_2^2 + (\rho - \tau\beta_H)\psi_2 + \mu_2(2\rho + \psi_2)\right)\right)},\ A_{10} = \frac{(\beta_H\eta_4\pi_1)}{(\theta_2\mu_1 K_V)},$$

$$A_9 = \frac{\pi_1\beta_H\mu_2\left(\tau\beta_H\theta_2\xi_1\psi_2 + \eta_3\theta_2\left(\rho^2 + \mu_2^2 + (\rho - \tau\beta_H)\psi_2 + \mu_2(2\rho + \psi_2)\right) + \eta_4\theta_3\left(\rho^2 + \mu_2^2 + (\rho - \tau\beta_H)\psi_2 + \mu_2(2\rho + \psi_2)\right)\right)}{\theta_2\mu_1\left(-\tau\pi_2\beta_H\xi_1\varphi_3\psi_2 + K_V(\theta_2 + \theta_3)\mu_2\left(\rho^2 + \mu_2^2 + (\rho - \tau\beta_H)\psi_2 + \mu_2(2\rho + \psi_2)\right)\right)}.$$

This value of v_2 and w_2 satisfies the given property. We now calculate the second order partial derivatives of g_i at the disease free equilibrium E_0 to get

$$\frac{\partial^2 g_2}{\partial x_1 \partial x_8} = \frac{\beta_H \mu_2}{\pi_2}, \quad \frac{\partial^2 g_2}{\partial x_1 \partial x_9} = \frac{\beta_H \eta_3}{K_V}, \quad \frac{\partial^2 g_2}{\partial x_1 \partial x_{10}} = \frac{\beta_H \eta_4}{K_V}, \quad \frac{\partial^2 g_2}{\partial x_2 \partial x_3} = \frac{-\beta_H \eta_2 \mu_1}{\pi_1},$$

$$\frac{\partial^2 g_2}{\partial x_2 \partial x_4} = \frac{-\beta_H \eta_1 \mu_1}{\pi_1}, \quad \frac{\partial^2 g_2}{\partial x_3 \partial x_4} = \frac{-\beta_H \mu_1 (\eta_1 + \eta_2)}{\pi_1}, \quad \frac{\partial^2 g_2}{\partial x_3 \partial x_5} = \frac{-\beta_H \eta_2 \mu_1}{\pi_1}, \quad \frac{\partial^2 g_2}{\partial x_3 \partial x_3} = \frac{-2\beta_H \eta_2 \mu_1}{\pi_1},$$

$$\frac{\partial^2 g_2}{\partial x_4 \partial x_4} = \frac{-2\beta_H \eta_1 \mu_1}{\pi_1}, \quad \frac{\partial^2 g_2}{\partial x_4 \partial x_5} = \frac{-\beta_H \eta_1 \mu_1}{\pi_1}, \quad \frac{\partial^2 g_2}{\partial x_6 \partial x_8} = \frac{-\beta_H \pi_1 \mu_2^2}{\pi_2^2 \mu_1}, \quad \frac{\partial^2 g_2}{\partial x_7 \partial x_8} = \frac{-\beta_H \pi_1 \mu_2^2}{\pi_2^2 \mu_1},$$

$$\frac{\partial^2 g_2}{\partial x_8 \partial x_8} = \frac{-2\beta_H \pi_1 \mu_2^2}{\pi_2^2 \mu_1}, \quad \frac{\partial^2 g_7}{\partial x_7 \partial x_8} = \frac{-\beta_H \mu_2}{\pi_2}, \quad \frac{\partial^2 g_7}{\partial x_8 \partial x_8} = \frac{-2\beta_H \mu_2}{\pi_2}, \quad \frac{\partial^2 g_7}{\partial x_6 \partial x_9} = \frac{\beta_H \xi_1}{K_V}.$$

We now compute the values of a and b to get

$$
\begin{aligned}
a &= \sum_{k,i,j=1}^{10} v_k w_i w_j \frac{\partial^2 g_k(0,0)}{\partial x_i \partial x_j} \\
&= \left[\frac{\beta_H \eta_3}{K_V} w_9 + \frac{\beta_H \eta_4}{K_V} w_{10} \right] v_2 w_1 + \left(\frac{\beta_H \xi_1}{K_V} \right) v_7 w_6 w_9, \\
&- \frac{\beta_H \eta_2 \mu_1}{\pi_1} [w_2 + w_5 + 2w_3 + w_4] v_2 w_3 - \frac{\beta_H \mu_2}{\pi_2} [w_7 + 2w_8] v_7 w_8, \\
&- [w_7 + 2w_8] v_2 w_8 - \frac{\beta_H \eta_1 \mu_1}{\pi_1} [w_2 + w_3 + 2w_4 + w_5] v_2 w_4, \\
&+ \frac{\beta_H \mu_2}{\pi_2} w_1 v_2 w_1 - \frac{\beta_H \pi_1 \mu_2^2}{\pi_2^2 \mu_1} w_6 v_2 w_8,
\end{aligned}
\tag{A.5}
$$

and

$$
\begin{aligned}
b &= \sum_{k,i=1}^{10} v_k w_i \frac{\partial^2 g_k(0,0)}{\partial x_i \partial \beta_H} \\
&= v_2 w_3 \eta_2 + v_2 w_4 \eta_1 + v_2 w_8 \frac{\pi_1 \mu_2}{\pi_2 \mu_1} + v_2 w_9 \frac{\pi_1 \eta_3}{\mu_1 K_V} + v_2 w_{10} \frac{\pi_1 \eta_4}{\mu_1 K_V} + v_7 w_8 + v_7 w_9 \frac{\pi_2 \xi_1}{\mu_2 K_V} > 0.
\end{aligned}
\tag{A.6}
$$

(i) If $\frac{\beta_H \mu_2}{\pi_2} w_1 v_2 w_1 < \frac{\beta_H \pi_1 \mu_2^2}{\pi_2^2 \mu_1} w_6 v_2 w_8$ and $b > 0$, then system (5) will undergo a forward bifurcation at $R_0 = 1$.

(ii) If $B_{wv} < \frac{\beta_H \mu_2}{\pi_2} w_1 v_2 w_1 - \frac{\beta_H \pi_1 \mu_2^2}{\pi_2^2 \mu_1} w_6 v_2 w_8$, and $b > 0$, then system (5) will undergo a backward bifurcation at $R_0 = 1$, where

$$
\begin{aligned}
B_{wv} &= \left[\frac{\beta_H \eta_3}{K_V} w_9 + \frac{\beta_H \eta_4}{K_V} w_{10} \right] v_2 w_1 + \left(\frac{\beta_H \xi_1}{K_V} \right) v_7 w_6 w_9 - \frac{\beta_H \eta_2 \mu_1}{\pi_1} [w_2 + w_5 + 2w_3 + w_4] v_2 w_3, \\
&- \frac{\beta_H \mu_2}{\pi_2} [w_7 + 2w_8] v_7 w_8 - [w_7 + 2w_8] v_2 w_8 - \frac{\beta_H \eta_1 \mu_1}{\pi_1} [w_2 + w_3 + 2w_4 + w_5] v_2 w_4.
\end{aligned}
\tag{A.6}
$$

References

Abdulhamid, A., Hussaini, N., Musa, S. S., & He, D. (2022). Mathematical analysis of lassa fever epidemic with effects of environmental transmission. *Results in Physics, 35*, Article 105335.

ACDC. (2018). Lassa fever. Report on lassa fever: Centre for disease control and prevention. Retrieved on 21-04-2021 from https://africacdc.org/disease/lassa-fever/.

Akhmetzhanov, A. R., Asai, Y., & Nishiura, H. (2019). Quantifying the seasonal drivers of transmission for lassa fever in Nigeria. *Philosophical Transactions of the Royal Society B, 374*, Article 20180268.

Bausch, D. G., Hadi, C. M., Khan, S. H., & Lertora, J. J. (2010). Review of the literature and proposed guidelines for the use of oral ribavirin as postexposure prophylaxis for lassa fever. *Clinical Infectious Diseases, 51*, 1435–1441.

Blower, S. M., & Dowlatabadi, H. (1994). Sensitivity and uncertainty analysis of complex models of disease transmission: An hiv model, as an example. *International Statistical Review/Revue Internationale de Statistique*, 229–243.

Castillo-Chavez, C., Feng, Z., Huang, W., et al. (2002). On the computation of ro and its role on. *Mathematical approaches for emerging and reemerging infectious diseases: An Introduction, 1*, 229.

Castillo-Chavez, C., & Song, B. (2004). Dynamical models of tuberculosis and their applications. *Mathematical Biosciences and Engineering, 1*, 361.

CDC. (2014). Lassa fever transmission. Report on viral hemorrhagic fevers: US department of health and human services. from https://www.cdc.gov/vhf/lassa/transmission/index.html. (Accessed 21 April 2021).

Chitnis, N., Hyman, J. M., & Cushing, J. M. (2008). Determining important parameters in the spread of malaria through the sensitivity analysis of a mathematical model. *Bulletin of Mathematical Biology, 70*, 1272–1296.

Control, P. P. (2018). How fast do mice multiply in your home? Preventive pest control. Retrieved on 21-02-2022 from https://www.preventivepesthouston.com/blog/2018/may/how-fast-do-mice-multiply-in-your-home-/.

Davies, J., Lokuge, K., & Glass, K. (2019). Routine and pulse vaccination for lassa virus could reduce high levels of endemic disease: A mathematical modelling study. *Vaccine, 37*, 3451–3456.

Fichet-Calvet, E., Becker-Ziaja, B., Koivogui, L., & Günther, S. (2014). Lassa serology in natural populations of rodents and horizontal transmission. *Vector Borne and Zoonotic Diseases, 14*, 665–674.

Freedman, H. I., Ruan, S., & Tang, M. (1994). Uniform persistence and flows near a closed positively invariant set. *Journal of Dynamics and Differential Equations, 6*, 583–600.

Gibb, R., Moses, L. M., Redding, D. W., & Jones, K. E. (2017). Understanding the cryptic nature of lassa fever in west africa. *Pathogens and Global Health, 111*, 276–288.

Gonzalez, S. G. (2020). Lassa fever. MedicineNet. Retrieved on 21-04-2021 from https://www.medicinenet.com/lassa_fever/article.htm.

Ibrahim, M. A., & Dénes, A. (2021). A mathematical model for lassa fever transmission dynamics in a seasonal environment with a view to the 2017–20 epidemic in Nigeria. *Nonlinear Analysis: Real World Applications, 60*, Article 103310.

Lakshmikantham, V., Leela, S., & Martynyuk, A. A. (1989). *Stability analysis of nonlinear systems*. Springer.

Ledder, G. (2017). Scaling for dynamical systems in biology. *Bulletin of Mathematical Biology, 79*, 2747–2772.

Lehmann, C., Kochanek, M., Abdulla, D., Becker, S., Böll, B., Bunte, A., Cadar, D., Dormann, A., Eickmann, M., Emmerich, P., et al. (2017). Control measures following a case of imported lassa fever from Togo, north rhine westphalia, Germany, 2016. *Euro Surveillance, 22*, 17–88.

Li, M. Y., & Muldowney, J. S. (1996). A geometric approach to global-stability problems. *SIAM Journal on Mathematical Analysis, 27*, 1070–1083.

Lo Iacono, G., Cunningham, A. A., Fichet-Calvet, E., Garry, R. F., Grant, D. S., Khan, S. H., Leach, M., Moses, L. M., Schieffelin, J. S., Shaffer, J. G., et al. (2015). Using modelling to disentangle the relative contributions of zoonotic and anthroponotic transmission: The case of lassa fever. *PLoS Neglected Tropical Diseases, 9*, e3398.

Marino, S., Hogue, I. B., Ray, C. J., & Kirschner, D. E. (2008). A methodology for performing global uncertainty and sensitivity analysis in systems biology. *Journal of Theoretical Biology, 254*, 178–196.

Mikucki, M. A. (2012). *Sensitivity analysis of the basic reproduction number and other quantities for infectious disease models*. Ph.D. thesis. Colorado State University.

Moghadas, S. M., Gumel, A. B., McLeod, R. G., & Gordon, R. (2003). Could condoms stop the aids epidemic? *Journal of Theoretical Medicine, 5*, 171–181.

Muldowney, J. S. (1990). Compound matrices and ordinary differential equations. *Rocky Mountain Journal of Mathematics*, 857–872.

Musa, S. S., Yusuf, A., Abdullahi, Z. U., Adamu, L., Mustapha, U. T., & He, D. (2022). *Unravelling the dynamics of lassa fever transmission with differential infectivity: Modeling analysis and control strategies*.

Musa, S. S., Zhao, S., Gao, D., Lin, Q., Chowell, G., & He, D. (2020). Mechanistic modelling of the large-scale lassa fever epidemics in Nigeria from 2016 to 2019. *Journal of Theoretical Biology, 493*, Article 110209.

NCDC. (2021). An update of lassa fever outbreak in Nigeria. Weekly Report on Lassa fever outbreak in Nigeria. Retrieved on 19-11-2021 from https://www.ncdc.gov.ng/diseases/sitreps/.

NCDC. (2022). An update of lassa fever outbreak in Nigeria. Weekly Report on Lassa fever outbreak in Nigeria. Retrieved on 15-03-2022 from https://www.ncdc.gov.ng/diseases/sitreps/.

Newman, T. (2018). *Everything you need to know about lassa fever. MedicalNewsToday*. from https://www.medicalnewstoday.com/articles/306886. (Accessed 21 April 2021).

NICD. (2020). Lassa fever disease. Lassa fever report: Division of the national health laboratory service. Retrieved on 21-04-2021 from https://www.nicd.ac.za/diseases-a-z-index/lassa-fever/.

Obabiyi, O., & Onifade, A. A. (2017). Mathematical model for lassa fever transmission dynamics with variable human and reservoir population. *International Journal of Differential Equations and Applications, 16*.

Ojo, M. M., Gbadamosi, B., Benson, T. O., Adebimpe, O., & Georgina, A. (2021). Modeling the dynamics of lassa fever in Nigeria. *Journal of the Egyptian Mathematical Society, 29*, 1–19.

Onah, I. S., Collins, O. C., Madueme, P. G. U., & Mbah, G. C. E. (2020). Dynamical system analysis and optimal control measures of lassa fever disease model. *International Journal of Mathematics and Mathematical Sciences, 2020*, Article 7923125.

Onuorah, M., Ojo, M., Usman, D., & Ademu, A. (2016). Basic reproductive number for the spread and control of lassa fever. *International Journal of Mathematics Trends and Technology, 30*, 1–7.

Ossai, E. N., Onwe, O. E., Okeagu, N. P., Ugwuoru, A. L., Eze, T. K., & Nwede, A. S. (2020). Knowledge and preventive practices against lassa fever among heads of households in abakaliki metropolis, southeast Nigeria: A cross-sectional study. *Proceedings of Singapore Healthcare, 29*, 73–80.

Peter, O. J., Abioye, A. I., Oguntolu, F. A., Owolabi, T. A., Ajisope, M. O., Zakari, A. G., & Shaba, T. G. (2020). Modelling and optimal control analysis of lassa fever disease. *Informatics in Medicine Unlocked, 20*, Article 100419.

Punch. (2022). Lassa fever kills four doctors, infects 38 health workers. PUNCH Newspaper, Retrieved on 15-03-2022 from https://punchng.com/lassa-fever-kills-four-doctors-infects-38-health-workers/.

Richmond, J. K., & Baglole, D. J. (2003). Lassa fever: Epidemiology, clinical features, and social consequences. *BMJ, 327*, 1271–1275.

Sabeti, P. C. (2015). *Clinical sequencing uncovers origins and evolution of lassa virus*. Cell.

Saltelli, A., Ratto, M., Andres, T., Campolongo, F., Cariboni, J., Gatelli, D., Saisana, M., & Tarantola, S. (2008). *Global sensitivity analysis: The primer*. John Wiley & Sons.

Saltelli, A., Tarantola, S., Campolongo, F., Ratto, M., et al. (2004). *Sensitivity analysis in practice: A guide to assessing scientific models* (Chichester, England).

Srivastava, A., Srivastava, P. K., et al. (2022). Nonlinear dynamics of a siri model incorporating the impact of information and saturated treatment with optimal control. *The European Physical Journal Plus, 137*, 1–25.

Stephenson, E. H., Larson, E. W., & Dominik, J. W. (1984). Effect of environmental factors on aerosol-induced lassa virus infection. *Journal of Medical Virology, 14*, 295–303.

Tewogbola, P., Aung, N., . Lassa fever: History, causes, effects, and reduction strategies. Virus 2, 16.

Trends, M. (2021). *Nigeria life expectancy 1951-2021. Macro Trends*. Retrieved on 19-11-2021 from https://www.macrotrends.net/countries/NGA/nigeria/life-expectancy.

Turányi, T. (1990). Sensitivity analysis of complex kinetic systems. tools and applications. *Journal of Mathematical Chemistry, 5*, 203–248.

Van den Driessche, P., & Watmough, J. (2002). Reproduction numbers and sub-threshold endemic equilibria for compartmental models of disease transmission. *Mathematical Biosciences, 180*, 29–48.

Velasco-Hernandez, J. X., & Hsieh, Y. H. (1994). Modelling the effect of treatment and behavioral change in hiv transmission dynamics. *Journal of Mathematical Biology, 32*, 233–249.

WHO. (2017). Lassa fever. WHO factsheets. from http://www.who.int/mediacentre/factsheets/fs179/en/. (Accessed 21 April 2021).

WHO. (2020). *Lassa fever-Nigeria*. WHO Factsheets. Retrieved on 21-04-2021 from https://www.who.int/csr/don/20-february-2020-lassa-fever-nigeria/en/.

WHO. (2021). *Stakeholders shore up sensitization campaign to curb lassa fever outbreak in edo state*. World Health Organization. Retrieved on 19-11-2021 from https://www.afro.who.int/news/stakeholders-shore-sensitization-campaign-curb-lassa-fever-outbreak-edo-state.

Yun, N. E., & Walker, D. H. (2012). Pathogenesis of lassa fever. *Viruses, 4*, 2031—2048.

Zhao, S., Musa, S. S., Fu, H., He, D., & Qin, J. (2020). Large-scale lassa fever outbreaks in Nigeria: Quantifying the association between disease reproduction number and local rainfall. *Epidemiology and Infection, 148*.